Reviews in Mineralogy & Geochemistry
Vol. 63, pp. 313-362, 2006

Neutron Scattering and Diffraction Studies of Fluids and Fluid-Solid Interactions

David R. Cole

Chemical Sciences Division
Oak Ridge National Laboratory
Oak Ridge, Tennessee 37831-6110, U.S.A.
e-mail: coledr@ornl.gov

Kenneth W. Herwig and Eugene Mamontov

Spallation Neutron Source
Oak Ridge National Laboratory
Oak Ridge, Tennessee 37831-6475, U.S.A.

John Z. Larese

Department of Chemistry
University of Tennessee
Knoxville, Tennessee, 37996, U.S.A.

INTRODUCTION

Role of fluids in earth systems with the focus on H_2O

Geologic fluids (defined liberally as gases, liquids, and supercritical solutions) act as reaction media, reactants, and carriers of energy and matter in the natural environment. Among the many different types of geologic fluids, those containing volatile C-O-H-N-S species and those enriched in chloride salts (brines) are of particular interest. They occur widely in varied geochemical settings, commonly contain significant quantities of dissolved and suspended compounds (complex hydrocarbons, organic macromolecules, colloids/nanoparticles), play a crucial role as primary reaction media, and are important sources and sinks of greenhouse gases. The consequences of coupled reactive-transport processes common to most geological environments depend on the properties and reactivities of these fluids over broad ranges of temperature, pressure and fluid composition. The relative strengths of complex molecular-scale interactions in geologic fluids, and the changes in those interactions with temperature, pressure, and fluid composition, are the fundamental basis for observed fluid properties. Understanding these solvent-mediated interactions for broad classes of solutes and suspensions in natural systems over the range of conditions typical of geologic fluids will greatly improve our capability to model and predict fluid behavior, reactivity, and the partitioning of elements and isotopes between coexisting species and phases.

Complex intermolecular interactions of C-O-H-N-S fluids (H_2O, CO_2, H_2, H_2S, N_2, CH_4) result in their unique thermophysical properties, including large deviations in the volumetric properties from ideality, vapor-liquid equilibria, and critical phenomena. Water is one of the best general solvents for inorganic materials due to its molecular structure and the distribution of electric charge (Neilson et al. 2002). In aqueous fluids containing various solutes (electrolytes, metals, organic/bio-molecules), numerous solute-solute and solute-solvent reactions lead to specific interactions, including complexation, binding, local ordering, and clustering. Indeed, a key goal in geochemistry is to develop a comprehensive understanding of the thermophysical

1529-6466/06/0063-0013$10.00 DOI: 10.2138/rmg.2006.63.13

properties, structures, dynamics, and reactivities of complex geologic fluids and molecules (water and other C-O-H-N-S fluids, electrolytes, and organic-biological molecules) at multiple length scales (molecular to macroscopic) over wide ranges of temperature, pressure, and composition. This knowledge is foundational to advances in the understanding of other geochemical processes involving mineral-fluid interfaces and reactions. It is also becoming increasingly clear that organic molecules in aqueous and mixed-volatile fluids—ranging from simple hydrocarbons and carboxylic acids to branched and cyclic compounds, to proteins and humic substances—play major roles in controlling geochemical processes, not just at the Earth's surface, but also deep within the crust. The origin of life may be partly attributable to the properties of such molecules in complex fluids under extreme conditions, as they appear to play an important role in mineral reactivity and templating of mineral precipitates.

Fluid/fluid and fluid/solid interfaces are regions across which all elemental transfers take place. The complex structural and dynamic changes that occur at interfaces can profoundly affect hydrodynamics, reaction rates and reaction mechanisms. Recently, there has been considerable effort devoted to behavior at 'stable' interfaces, involving the juxtaposition of phases that largely retain their bulk characteristics at some distance from the interface. This enables us to isolate the unique features of the interface, which are controlled in part by changes in the compositions and state conditions of the bulk phases, whose structural and dynamic properties are often better understood (e.g., Brown et al. 1999; Wesolowski et al. 2004).

Nanoscale porosity can be generated from structural modifications (Radlinski 2006, this volume) in a reaction zone, and this process can be understood by correlating the extent and rate of change of chemical and isotopic signatures with contemporaneous structural modifications. Confinement of fluids in the porous reaction (leached) zones can impact fluid-phase behavior, chemical transport across the zone, and reactivity. A molecular-level understanding of the reactive interface between the product and parent phases is starting to yield a more predictive view of time- and state-dependent reaction progress (e.g., Cole et al. 2004).

Finally, the importance of water in deep earth and planetary processes even at trace levels, cannot be overstated (Williams and Hemley 2001). Water affects physical and chemical processes such as melting, mantle convection and the chemistry of melts generated from the earth's mantle. How water is stored in the earth, what the water content of mineral phases is, and how it is mobilized are key issues addressed by numerous methodologies, not the least of which involves the use of neutron scattering and diffraction.

Why neutrons – hydrogen (and deuterium) is the key?

Given the complexity of natural geo-fluids and their role in mediating surface interactions and reactivity with mineral phases, there can be no doubt that a quantitative understanding is needed of molecular-level fluid properties and fluid interactions with solids. There is a wide spectrum of analytical approaches that can be brought to bear, including, but certainly not limited to dynamic light scattering, IR, microscopy (e.g., electron; force), NMR, synchrotron-based X-rays, and neutron scattering and diffraction. When coupled with molecular simulation, this wide array of methods provides the means by which we can interrogate the structure and dynamics of fluids and their interactions with solids. Each of these provides a unique window into the properties and behavior of fluids and their reactivity.

Neutron and X-ray scattering are two of the most important tools available to probe the atomic structure of fluids, including aqueous solutions and complex liquids. Scattering patterns obtained experimentally and the distribution function, $g(r)$, are related through Fourier transformation (e.g., Nielson et al. 2002). Interatomic distances, coordination numbers and the extent of local order around a particular atom can be delineated through a quantitative understanding of distribution functions, either individually, or as combinations ($G_\alpha(r)$) specific to a particular atom (or ion; α or β), or as total fluctuations ($G(r)$), of all species in the fluid.

The local structure can be divided into several parts such as the contact distance, next nearest neighbor distance, etc., and eventually the end of short-range order (see Fig. 3 in Wilding and Benmore 2006, this volume). Furthermore, from an examination of the shapes of the correlation in $g(r)$, one can obtain a qualitative guide to the degree of complexation (Nielson and Adya 1997). Experimental structural information can be used to assess the interatomic correlations in all types of fluids, and to test the robustness of simulations based on model potentials for specific components.

There are a number of distinct advantages in using neutrons and X-rays to determine the structure of fluids, glasses and other amorphous materials (see also Wilding and Benmore 2006). The principal advantage of neutron methods stems from the fact that neutrons interact directly with the atomic nuclei within a molecule through the strong force and the interaction is isotropic. Consequently, structural information in the form of $g_{\alpha\beta}(r)$ is accessible directly from the experimental diffraction data. The strength of this interaction varies irregularly with atomic number, so that even isotopes of the same element do not have the same neutron scattering cross-section or scattering length. For example, as shown in Table 1, the most significant isotopic variation occurs for hydrogen, which has a coherent scattering length of −3.74 barn, whereas for deuterium the scattering length is 6.67 barn. Therefore, two fluids with the same composition of atoms but containing isotopically different nuclei (e.g., CH_4 vs. CD_4; $H^{35}Cl$ vs. $H^{37}Cl$, etc.) will yield different neutron scattering patterns. The fact that neutrons are sensitive to hydrogen and differences between its isotopes permits observation and measurement of the hydrogen structural correlations in water (and other hydrogeneous phases) that are not easily obtainable by X-rays. In contrast to X-rays, neutrons are coherently scattered equally strongly by light and heavy elements—i.e., hydrogen scatters coherently just as effectively as manganese. Hence, neutrons can be used to probe the structure of molecules containing lighter atoms. We will see later in this chapter that isotopic substitution will play a pivotal role in determination of structural features of both simple fluids (e.g., H_2O) as well as more complex solutions such as electrolyte-bearing waters.

One final aspect of neutron interaction with fluids is worth discussing. The isotopic compositions of molecular species can be tailored such that their scattering or diffraction properties differ from one another and from solid matrices with which they may be interacting.

Table 1. Coherent scattering lengths (fm[a]) of important elements common to fluids found on and within the Earth (from Enderby et al. 1987).

Element or Isotope	*b*	Element or Isotope	*b*	Element or Isotope	*b*
H	−3.74	^{40}Ca	4.9	^{65}Cu	11.1
D	6.67	^{44}Ca	1.8	Zn	5.686
^{6}Li	1.87	Fe	9.51	^{64}Zn	5.5
^{7}Li	−2.2	^{54}Fe	4.2	^{68}Zn	6.7
N	9.36	^{56}Fe	10.1	Ag	5.97
^{14}N	9.37	^{57}Fe	2.3	^{107}Ag	7.64
^{15}N	6.44	Ni	10.3	^{109}Ag	4.19
K	3.67	^{58}Ni	14.4	^{113}In	5.39
^{41}K	2.58	^{60}Ni	2.82	^{115}In	4.00
Cl	9.58	^{62}Ni	−8.7	Ba	5.07
^{35}Cl	11.7	^{64}Ni	−0.37	^{130}Ba	−3.6
^{37}Cl	3.1	Cu	7.718	^{137}Ba	6.82
Ca	4.9	^{63}Cu	6.7		

[a]1 fm = 10^{-15} m

Hence, neutron scattering and diffraction permits interrogation of the structure and dynamics of fluids at interfaces and within confined geometries. The behavior of fluids at interfaces or in confinement commonly differs from their bulk behavior in interesting, and not necessarily intuitive, ways. For example, how water (and other fluid species) orients and moves near and on a mineral (or biomolecular) surface or within a nanopore can be addressed by neutron techniques which are non-invasive and nondestructive (e.g., Mamontov 2004, 2005). Indeed, a number of neutron methods exist that allow the study of fluid structural properties involving translational as well as orientational ordering of fluids on surfaces or within micro- or mesoporous materials (Idziak and Li 1998). These topics will be discussed in detail later in this chapter.

Important molecular-level behavior amenable to neutron scattering and diffraction

While it is clear that no one method can sufficiently resolve structure at the required level around all species in bulk complex fluids or fluids interacting with an interface, neutrons do provide a unique probe useful in approaching certain aspects of a number of key molecular issues. One prime example involves the phenomenon of *hydrogen bonding* which plays a fundamental role in the structure, function and properties of many fluids of geochemical and biogeochemical importance. The interaction manifests itself as a pronounced, directional correlation between specific sites on neighboring molecules (Bruni et al. 1996). It also produces a highly characteristic vibrational density of states in hydrogen bonded molecules, and dramatically affects the thermodynamic properties of a fluid compared to what they would be if the molecules interacted simply by van der Waals interactions. In crystalline materials the hydrogen-bond direction will relate to some aspect of the crystal symmetry, but in disordered fluids and materials the ordering effect of the orientational correlations is influenced by the inherent disorder of the molecular arrangement (Dore 1991). The complexity of hydrogen-bonded networks poses many problems that have still not been resolved and arguments persist over the true cause of the hydrogen bond interaction. In fact, the question of how many bonds each H_2O molecule makes with its nearest neighbor was identified as one of the top 125 fundamental science questions (Kennedy and Norman 2005).

Perturbation of hydrogen-bonding and associated molecular fluid structures may arise from either the presence of dissolved constituents (e.g., solutes in aqueous solution) or interfacial interactions between a fluid and a solid such as a colloid or nanoparticle, a 2D mineral surface, or within a porous or highly fractured network. A molecular-level understanding of the nature of speciation of solutes in aqueous solution is a critical question with direct impact on the quantities such as solid solubilities and the alteration of geological materials. Neutron diffraction with isotopic substitution (NDIS) permits the direct determination of radial distribution functions $g_{\alpha\beta}(r)$, providing the appropriate level of molecular-level structural detail. Small-angle neutron scattering and diffraction can also be employed in real-time studies of the nucleation and assembly of macromolecules (e.g., biopolymers, including proteins) and low-dimensional building blocks that give rise to crystalline nanoparticles. *In situ*, non-invasive neutron methods permit interrogation of poorly constrained mechanisms of transformation of a mixture of solid and fluid components into a complex extended solid (Walton et al. 1999, 2002). Neutron scattering techniques are ideally suited for the study of the structure and dynamics of atoms and molecules physisorbed on surfaces (e.g., Larese 1997, 1999) including processes such as multi-layer development, melting and rotational tunneling on unreactive stable surfaces. Furthermore, structural and dynamical features associated with chemisorption involving the formation of surface hydroxyl groups that saturate the coordination of surface cations and complete the interrupted bulk crystalline network can be "imaged" by neutron methods. The dynamical behavior of fluids and gases contained within porous solids is controlled by processes occurring at the interface as well as the rates of supply and removal of mobile components. The richness and complexity of fluid behavior (e.g., phase transitions, molecular orientation and relaxation, diffusion, adsorption, wetting,

capillary condensation, etc.) in confined geometries has been, and continues to be, the focus of numerous applications of neutron scattering.

Objectives

The focus of this chapter is the application of neutron scattering and diffraction methods to the study of fluids and their interaction with solid matrices. By way of numerous examples, emphasis is placed on what neutrons can tell us about the molecular-level properties and behavior of geo-fluids and the processes attendant with their interaction with solid surfaces. Discussion focuses on two main themes, homogeneous fluids with a major emphasis on both water and aqueous solutions containing dissolved constituents, and the structure and dynamics of fluids interacting with either solid surfaces or within confined geometries, again with an emphasis on water. While we recognize the increased importance of inorganic-organic-biologic interactions, particularly at surface and near-surface earth conditions, the review of the complex molecular interplay of these chemical systems is unfortunately beyond the scope of this review.

HOMOGENEOUS FLUIDS

Background

The structure of pure liquids, such as water, and aqueous solutions is conveniently interrogated using scattering techniques. The most common of these includes the use of either X-rays or neutrons. Differences arise due to the variations in the scattering properties of single atoms for each kind of radiation. In either case, radiation penetrates the liquid and is scattered through an angle θ. Analytical information is obtained by assessing the intensity of the scattered radiation as a function of this angle. The scattering of radiation by condensed matter may be related to the distribution of atomic positions if the wavelength λ of the radiation is of the order of magnitude of the interatomic spacing r. The distribution of scattering intensity contains information on the distribution of atoms, and the measured spectrum of energy transfer contains information on single and collective particle motion. A major goal in the study of fluids is to identify and test the relationship between intermolecular forces and the microscopic structure and dynamics of the fluids. Understanding the structure and dynamics of bulk fluids is a prerequisite to studying these for fluids interacting with surfaces or confined to porous matrices. The following discussion of the basic principles of neutron scattering in liquids is intended to complement the description provided in Loong (2006, this volume) and Wilding and Benmore (2006, this volume) with emphasis placed here on a description of structure and dynamics of water and aqueous solutions containing inorganic solutes.

The neutrons used in a neutron scattering experiment penetrate matter rather easily. Unlike X-rays which are scattered by electromagnetic interaction with the atomic electron distribution, the neutron is scattered by the nucleus which behaves as a point scatter since its size ($\sim 10^{-15}$ m) is much smaller than the wavelength of the incident neutron ($\sim 10^{-10}$ m). The essential features of the scattering pattern are related to a structure factor that characterizes the basic arrangement of scattering centers for the fluid under investigation. In ordered materials, such as crystals, the regular arrangement of the lattice leads to a series of well-defined peaks governed by the Laue conditions. By contrast, scattering in partially disordered materials such as fluids or amorphous solids produces patterns composed of broad oscillatory structures which still contain structural information through the phase differences arising from interference of the scattered waves. The formalism for describing the scattering of neutrons is much simpler than that for X-rays because there is no need to introduce an atomic scattering factor to represent the spatial distribution for each individual scattering unit. There are, however, other characteristics arising from the mechanism of nuclear interaction that must be accounted for and have a significant bearing on the design of experiments and interpretation of results.

Scattering experiments fall into two categories (Winter 1993). The first involves experiments where only the angular distribution of the scattering intensity is determined, and the second considers both the angular distribution for the intensity and the energy transfer. In the former, the intensity is related to the static structure factor $S(Q)$, and in the latter the intensity is related to the dynamic structure factor $S(Q,E)$, where $\mathbf{Q}$ and E are the momentum and energy transferred to the particle in the scattering process, respectively. The direction of a wave vector is the direction of propagation of the plane wave and its magnitude is $2\pi/\lambda$. The incoming radiation in the experiment is characterized by its wavelength, λ and by its intensity, I_o. The λ is chosen so that it is commensurate with the average distance between atoms, but much smaller than the sample dimensions.

Scattering theory

In the context of water, Wilding and Benmore (2006, this volume) provide a fairly complete description of scattering theory, experimental methodologies and various corrections attendant with neutron diffraction. Our intent here is only to amplify and where necessary, expand a bit on some of the concepts that were introduced. Neutron diffraction concerns the measurement of the coherent interference of scattered waves. The experimental method may be monochromatic angle-dispersive (typically reactor based) or time-of-flight energy-dispersive (typically based at a pulsed source). Diffraction experiments probe the differential cross (DC) section of neutrons (Egelstaff 1992), $d\sigma/d\Omega$, defined as the ratio of the scattering cross (SC) section $d\sigma$ scattered into the solid angle $d\Omega$ about the scattering angle θ. For an assembly of fixed nuclei (forming molecules or not) the DC is described by the static approximation:

$$\frac{d\sigma}{d\Omega} = \frac{1}{N}\sum_{\alpha,\beta}\bar{b}_\alpha\bar{b}_\beta\left\langle e^{-i\mathbf{Q}\cdot\mathbf{r}_\alpha}\, e^{-i\mathbf{Q}\cdot\mathbf{r}_\beta}\right\rangle \tag{1}$$

where $\bar{b}_i$ is the coherent scattering length associated with the nucleus with position $\boldsymbol{r}_i$. The operators $\boldsymbol{r}_\alpha$ and $\boldsymbol{r}_\beta$ are assumed to both be evaluated at $t = 0$ according to the Heisenberg convention inside the thermal expectation bracket. For a complete evaluation of Equation (1) we assume that all relevant energy transfers have been integrated over the momentum transfer for the elastic process for the given $\mathbf{Q}$, and that N is the total number of scatterers in the sample. A variety of corrections to experimental data are required accounting for effects such as incoherent and multiple scattering, inelastic effects, container absorption, etc (Head-Gordon and Hura 2002; Wilding and Benmore 2006, this volume). This cross section may be split into a self ($\alpha = \beta$) and distinct (coherent interference) part:

$$\frac{d\sigma}{d\Omega} = \left(\frac{d\sigma}{d\Omega}\right)^{self} + \left(\frac{d\sigma}{d\Omega}\right)^{distinct} \tag{2}$$

The advantage of this division of the SC is to isolate the unwanted effect of incoherent scattering into the self term. The self part can be further split into self-coherent and an incoherent part:

$$\left(\frac{d\sigma}{d\Omega}\right)^{self} = \left(\frac{d\sigma}{d\Omega}\right)^{self}_{coh} + \left(\frac{d\sigma}{d\Omega}\right)_{incoh} \tag{3}$$

In the case of water, the contribution of incoherent scattering comes from either hydrogen or deuterium since the incoherent cross-section of oxygen is virtually zero. Using D_2O in scattering experiments avoids the large contribution of incoherent scattering from hydrogen to the unwanted background of structural measurements. In the case of pure D_2O

$$\left(\frac{d\sigma}{d\Omega}\right)^{self} = \left(b_O^2 + 2b_D^2\right) + 2\left(\frac{\sigma_{D,incoh}}{4\pi}\right) \tag{4}$$

where b_O and b_D are the coherent scattering lengths for oxygen and deuterium atoms, respectively, b_O = 5.85 barn, b_D = 6.674 barn, and where $\sigma_{D,incoh}$ = 2.032 barn is the incoherent scattering cross section due to deuterium atoms D. The distinct part can be separated into an intra- and inter-molecular part corresponding to correlations between atoms in the same molecule or atoms belonging to different molecules, respectively:

$$\left(\frac{d\sigma}{d\Omega}\right)^{distinct} = \left(\frac{d\sigma}{d\Omega}\right)^{intra} + \left(\frac{d\sigma}{d\Omega}\right)^{inter} \qquad (5)$$

Thus, the DC may now be expressed by the relation:

$$\left(\frac{d\sigma}{d\Omega}\right) = \left(\frac{d\sigma}{d\Omega}\right)^{self} + \left(\frac{d\sigma}{d\Omega}\right)^{intra} + \left(\frac{d\sigma}{d\Omega}\right)^{inter} \qquad (6)$$

The intensity of scattering for molecular systems is converted to a normalized molecular structure factor, $S_M(Q)$ where **Q** is the elastic scattering vector (Fig. 1). The $S(Q)$ is directly related to the distinct part of the DC which for D_2O is given as:

$$S_M(\mathbf{Q}) = \frac{\left(d\sigma/d\Omega\right)^{distinct} + \left(b_O^2 + 2b_D^2\right)}{\left(b_O + 2b_D\right)^2} \qquad (7)$$

For a molecular fluid like D_2O or H_2O, it is convenient to separate terms into those arising from correlations in the same molecule (intramolecular terms) and those from correlations in different molecules (intermolecular terms). Thus the structure factor may be split into two parts as:

$$S_M(Q) = f_1(Q) + D_M(Q) \qquad (8)$$

where $f_1(Q)$ is the molecular form factor and the $D_M(Q)$ function contains all of the intermolecular correlations. The $f_1(Q)$ function is equivalent to the diffraction pattern that would be observed for individual molecules in the low-density regime and it is solely dependent on the molecular conformation and coherent scattering lengths of the constituents. For D_2O molecules this becomes (Dore 1985):

$$\left[f_1(Q)\right]^{D_2O} = \frac{1}{\left(b_O + 2b_D\right)^2}\left[b_O^2 + 2b_D^2 + 4b_O b_D F\left(Q, r_{OD}\right) + 2b_D^2 F\left(Q, r_{DD}\right)\right] \qquad (9a)$$

where r_{OD} *i*s the bond length and $r_{DD} = 2r_{OD}\sin\theta/2$ for an intramolecular bend angle, θ, and:

$$F(Qr_{\alpha\beta}) = \frac{\sin Qr_{\alpha\beta}}{Qr_{\alpha\beta}} \exp(-Q^2 u_{\alpha\beta}^2/2) \qquad (9b)$$

is the interference term; $u_{\alpha\beta}^2$ is the square amplitude of vibration for the distance $r_{\alpha\beta}$. The exponential term is an effective Debye-Waller factor that allows for variation of the time-

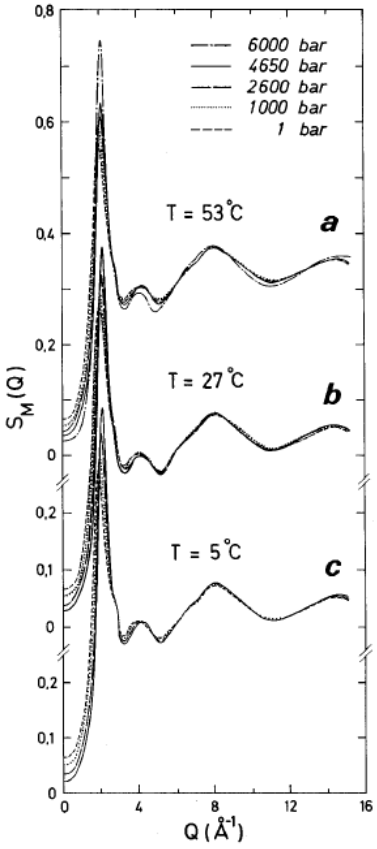

Figure 1. Examples of $S_M(Q)$ for D_2O obtained at three constant temperatures and pressures. (a) 53 °C, (b) 27 °C, (c) 5 °C. [Used by permission of American Physical Society, from Bellissent-Funel and Bosio (1995), J Chem Phys, Vol. 102, Fig. 4, p.3721]

averaged bond distance arising from thermal vibrations. The resulting *r*-parameter is an ensemble average over the thermally excited states of the molecule. The values of r_{OD} and r_{DD} may be used to define the mean bond-angle D···O···D for the water molecule in the liquid state (Dore et al. 2004).

In principle, at lower *Q*-values the difference term, $D_M(Q)$ contributes to the overall diffraction pattern and may be formally expressed as:

$$D_{\mathrm{M}}(Q) = \frac{1}{N_M\left[\sum b_n\right]^2}\left\langle \sum_{\alpha\neq\beta} \exp\left(\mathbf{Q}\cdot\mathbf{r}_{c_{\alpha\beta}}\right) \sum_{n_\alpha n_\beta} b_{n_\alpha} b_{n_\beta} \exp\left(\mathrm{i}\mathbf{Q}\cdot\left(\mathbf{r}_{c_{n,\alpha}} - \mathbf{r}_{c_{n,\beta}}\right)\right)\right\rangle \tag{10}$$

where *n* labels the nucleus within the molecule; α and β refer to different molecules in which the molecular center is situated; $\mathbf{r}_{cn}$ is the intramolecular distance of nucleus *n* from the molecular center and $\mathbf{r}_{c\alpha\beta}$ is the intermolecular distance between centers of molecules designated α and β. This function contains the required information on the spatial arrangement of the molecules in the fluid or glassy assembly as distinct from that of the molecule. The term "structure" corresponds to the ensemble average for all molecules in the system at a specific time. Since the fluid is composed of a large number of molecules in constant motion it is more convenient to think of this as a long-time average of the various changing configurations around a single molecule. The structure factor as defined in Equation (7) (and in Wilding and Benmore 2006, this volume) arises from an ensemble of snap shot images with a "shutter-speed" that is short compared to the characteristic motion of the scattering centers.

The most useful quantity for expressing the static structural characteristics of fluid order is the total pair correlation function, *g*(*r*) (Proffen 2006, this volume). This is related to the Fourier transform of *S*(*Q*) by the relation:

$$4\pi r\rho_M\left(g(r)-1\right) = \frac{2}{\pi}\int_0^\infty Q(S_M(Q)-S_M(\infty))\sin QrdQ \tag{11}$$

where $S_{\mathrm{M}}(\infty) = (b_{\mathrm{O}}^2 + 2b_{\mathrm{D}}^2)/(b_{\mathrm{O}} + 2b_{\mathrm{D}})^2$ is the asymptotic value of $f_1(Q)$ at large *Q* and ρ_{M} is the molecular density. The function *g*(*r*) is a combination of different partial (weighted) correlation functions and includes both inter- and intramolecular distances. In the case of water it is possible to remove the intramolecular terms by subtracting the molecular form factor from $S_{\mathrm{M}}(Q)$ to obtain $D_{\mathrm{M}}(Q)$, which may be Fourier transformed in order to obtain the pair correlation function $g_{\mathrm{L}}(r)$ for the intermolecular term only:

$$d_{\mathrm{L}}(r) = 4\pi r\rho_M\left(\mathrm{g}_{\mathrm{L}}(r)-1\right) = \frac{2}{\pi}\int_0^\infty QD_M(Q)\sin(Qr)dQ \tag{12}$$

Composite functions of this form will in general contain contributions from all the partial correlation functions weighted according to the *b*-values and relative concentrations, i.e.,

$$g_{\mathrm{L}}(r) = \sum c_\alpha^2 b_\alpha^2 \mathrm{g}_{\alpha\alpha}(r) + 2\sum_{\alpha\neq\beta} c_\alpha c_\beta b_\alpha b_\beta \mathrm{g}_{\alpha\beta}(r) \tag{13}$$

For neutron scattering by D_2O with two components we need to account for $n(n + 1)/2$ correlations, so the composite function is weighted with the following proportions:

$$g_{\mathrm{L}}(r) = 0.489\, g_{\mathrm{DD}}(r) + 0.421 g_{\mathrm{OD}}(r) + 0.090 g_{\mathrm{OO}}(r) \tag{14}$$

This result indicates that the signal is dominated by D-D and O-D correlations where D atoms make a significant contribution to the total scattering pattern in contrast to X-ray diffraction studies where it is the O atoms the predominate (Bellissent-Funel and Bosio 1995).

The measurement of the total coherent scattering intensity by means of a two- or three-

axis diffractometer (reactor source) or a time-of-flight spectrometer (pulsed source) enables the diffraction pattern to be obtained but careful data reduction incorporating experimental and analytical corrections is needed to normalize $S_M(Q)$ and $D_M(Q)$. Even for this simplest of cases, D_2O neutron diffraction, there is a need to account for a number of corrections. The major errors arise from inelasticity (Placzek correction), sample attenuation, multiple scattering, and absorption resonance (Wilding and Benmore 2006, this volume).

Difference methods

The structural information obtained from a single measurement does not necessarily provide much quantitative insight into the properties of the fluid although it can prove useful in checking the validity of simulation predictions from molecular dynamics or Monte Carlo methods. A more detailed study of a sample type such as H_2O can be achieved by isotopic substitution. In Wilding and Benmore (2006, this volume) the use of isotopic substitution to achieve either a *first-order* or *second-order difference function* from neutron diffraction was discussed. We will address these in more detail below as they apply to the interrogation of the structure of aqueous solutions containing dissolved ions. However, let us consider neutron diffraction isotope substitution (NDIS) in the context of our discussion of water. For H_2O, a similar expression to Equation (9a) can be used for the $f_1(Q)$ function with b_H instead of b_D. For isotopic mixtures, the effective coherent scattering is represented by the average value, $\langle b_{HD} \rangle = \alpha_D b_D + \alpha_H b_H$ where α_D is the mole fraction of deuterium [$\alpha_D + \alpha_H = 1$), provided it is assumed that the H and D atoms are in equivalent positions. The efficacy of the iso-structural assumption between light and heavy water has been documented extensively—e.g., Hart et al. (2005) and references therein.

From Table 2 we see that since $b_D = 6.67$ fm and $b_H = -3.74$ fm it is possible to change $\langle b_{HD} \rangle$ over a wide range and even to choose the special case of $\alpha_D = 0.359$ for which $\langle b_{HD} \rangle = 0$. The coherent and incoherent contributions for various mixtures of H_2O and D_2O are also given in Table 2. Soper and Egelstaff (1981) and Soper and Silver (1982) demonstrated that the technique of H-D substitution could be used to extract information on water structure. By performing three measurements on pure H_2O, pure D_2O, and a mixture (or more, as described by Dore et al. 2004) of H_2O and D_2O, one can exploit the scattering contrast of hydrogen

Table 2. Neutron parameters for various isotopes of hydrogen and oxygen, and the coherent and incoherent contributions for various H_2O/D_2O mixtures (Dore et al. 2004).

Neutron parameters for various isotopes of hydrogen and oxygen.				
	b/fm	σ_{coh}/barns	σ_{incoh}/barns	$\sigma_c\sigma_i$
H	−3.74	1.76	79.9	0.022
D	6.67	6.00	2.0	3.0
^{16}O	5.80	4.24	0	-
^{17}O	5.78	4.2	0.2	-
^{18}O	5.84	4.3	0	-

Coherent and incoherent contributions for various H_2O/D_2O mixtures.							
α_H	0	0.05	0.10	0.20	0.50	0.641	1.00
(b_{HD})/fm	6.67	6.15	5.63	4.59	1.47	0	−3.74
σ_{coh}	15.3	13.7	12.2	9.5	4.8	4.2	7.6
σ_{incoh}[H/D]	4.0	11.8	19.6	35.2	82	104	160
σ_{incoh}[mix]	0	1.3	2.4	4.2	6.6	7.6	0
$\Sigma\sigma_{incoh}$/mol	4.0	13.1	22.0	39.4	88.6	112	160
$\sigma_c\sigma_i$	3.8	1.05	0.47	0.24	0.054	0.037	0.048

and deuterium to isolate the three site-site correlation functions directly. If a 50:50 H/D mixture is used the inelastic contribution practically cancels in the data reduction process. This constitutes a *second-order difference* method which yields a total pair correlation function for each species as given by Wilding and Benmore (2006, this volume). These functions form the basis for calculating the partial pair distribution functions $g_{HH}(r)$, $g_{OH}(r)$, and $g_{OO}(r)$ examples of which are provided in Figure 2 for ambient conditions (Head-Gordon and Hura 2002). Modeling is required to provide a more complete 3D structural reconstruction of the pair correlation function which is a 1D representation. For fluids like water, the Empirical Potential Structural Refinement (EPSR) method summarized most recently by Soper (2005) provides one possible path to accomplish this.

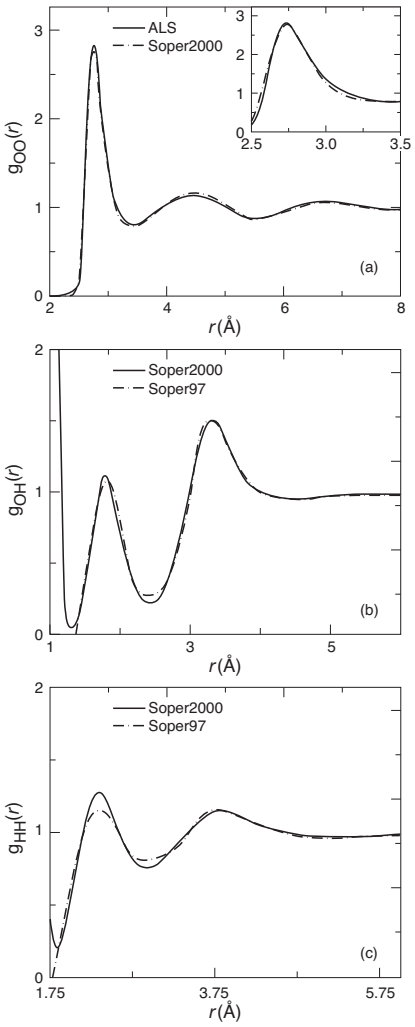

Figure 2. Comparison of neutron data (as $g(r)$) on pure water at 25 °C and 1 atm. (a) Comparison of ALS X-ray experimental $g_{OO}(r)$ from Hura et al. (2000), Sorenson et al. (2000) – solid line with reanalysis of Soper (2000) NDIS data (dashed line). Comparison of neutron data on pure water at 25 °C, 1 atm: Soper et al. (1997) – dot-dash line; Soper (2000) – solid line; for (b) $g_{OH}(r)$ and (c) $g_{HH}(r)$. [Used by permission of the American Chemical Society, from Head-Gordon and Hura (2002), Chem Rev, Vol. 102, Fig. 4a,b,c, p. 2661]

Structure of water at ambient and high temperature-pressure conditions

Ambient water. Despite the difficulties with the NDIS approach arising from the large uncertainty in the inelastic correction, numerous studies have been reported describing the use of this method to study water structure at ambient (e.g., Thiessen and Narten 1982; Soper and Philips 1986; Bruni et al. 1996; Soper et al. 1997; Ricci and Soper 2002) and elevated temperature and/or pressure conditions (e.g., Neilson et al. 1979; Gaballa and Neilson 1983; Ichikawa et al. 1991; Postorino et al. 1993; Tromp et al. 1994; Tassaing et al. 1998; Yamaguchi 1998; Soper 2000; Bellissent-Funel 2001). There are also numerous papers dealing with the subject of supercooled water which we have elected not to discuss in this section (e.g., Dore 1984, 1994; Bellissent-Funel et al. 1989; Bellissent-Funel 1998; Dore et al. 2000).

It is worth devoting some space to a discussion of the structure of bulk water to set the stage for perturbations produced by dissolved ions and the interactions with various types of solid interfaces to be described in later sections. Let us first consider the scattering amplitude for oxygen, which is smaller than that for hydrogen. Because the $g_{OO}(r)$ distribution is the most difficult to determine it is common for structural data from X-ray scattering to be used for comparison and incorporated

into simulation studies. Indeed, Soper (1996, 2000) reported new neutron analysis results based on previously obtained neutron diffraction data using the EPSR method where the $g_{OO}(r)$ is in very good agreement with X-ray scattering data reported by Hura et al. (2000) and Sorenson et al. (2000) as shown in Figure 2a. Head-Gordon and Hura (2002) point out that the use of the SPC/E water model for the reference potential by Soper probably helped improve this agreement. As Figure 2a shows the first peak gives us the first neighbor oxygen-oxygen distance which occurs at about 2.8 Å. Of special interest, however, is the estimate of the oxygen-oxygen coordination number which requires consideration of the distribution density over the whole region of the maximum in $g_{OO}(r)$. To do this, one can integrate the distribution function up to the first minimum, considering spherical shells of volume $4\pi r^2 dr$. The coordination number, n_C can then be described by:

$$n_c = 4\pi\rho_O \int_o^{r_{min}} g_{OO}(r) r^2 dr \tag{15}$$

where ρ_O is the density of oxygen atoms in the fluid and r_{min} is the location of the first minimum in $g_{OO}(r)$, which is roughly 3.5 Å. Depending on the NDIS data set, the n_C values can range from 4 to very close to 5. This coordination number depends critically upon the upper cut-off distance used in performing the interrogation under the peak (Finney and Soper 1994). Beyond the first minimum, $g_{OO}(r)$ oscillates with a second maximum at about 4.5 Å which corresponds to an O-O-O angle of about 110°. This is close to the tetrahedral angle, implying that the local water molecule geometry is on average tetrahedral, though the broad nature of the second nearest neighbor peak shows there is considerable variation around this average. Head-Gordon and Hura (2002) note the strict adherence to hydrogen-bonded hexagons of ice water give way to greater translational and rotational motion of waters and a broader distribution of hydrogen-bonded configurations, including a variety of polygons of varying sizes and degrees of puckering, or distortion, all of which result in a more compact arrangement of water molecules. Recent work by Wernet et al. (2004) based on X-ray scattering suggest that water exists in mixed form—two-hydrogen bonded (60-75%) and tetrahedral (25-40%) species.

A much different diffraction pattern is observed for the oxygen-hydrogen distribution function (Fig. 2b) where a very strong peak occurs at about 1 Å. This peak corresponds to the intramolecular O-H distance, and is a diagnostic indicator that the experiment is reporting correct results because it is located at the known OH distance with an area predicting two hydrogen atoms (Finney and Soper 1994). The second maximum is centered on about 1.85 Å and is associated with the hydrogen atoms in surrounding molecules that are hydrogen bonded to the oxygen atom in a central molecule—i.e., the intermolecular O-H. Integration out to the first minimum gives a coordination number of about 1.7 whereas this number becomes approximately 3.3 for the second peak integrated out to the second minimum. The third peak centered on about 3.25 Å occurs at the first minimum of the $g_{OO}(r)$ distribution curve and refers to non-hydrogen-bonded oxygen-hydrogen distances on neighboring molecules. At this point, the total number of hydrogen atoms around the central oxygen is close to eight which is two times the number of oxygens in the same volume of solution.

Finally, the distribution of hydrogen atoms with respect to a central hydrogen atom, the hydrogen-hydrogen $g_{HH}(r)$ correlation, is shown in Figure 2c. This function is the easiest to determine experimentally because of the large difference in scattering length for hydrogen and deuterium. The first peak (not shown) is at the intramolecular H-H distance of 1.55 Å and again confirms the molecular geometry of the water molecule. The second peak is just above 2.4 Å and represents the closest H-H distances between hydrogen-bonded neighbors. The coordination number calculated by integration out to the second minimum at 3.1 Å is roughly 5.8. The third broad, asymmetric peak occurs around 3.7-3.8 Å and refers to the distant H-H distances on neighboring water molecules. Comparing $g_{OH}(r)$ and $g_{OO}(r)$, we see

that the maxima on the H-H distribution function are located further from the central atom by 0.6 Å with respect to those on the O-H distribution (Fawcett 2004). This is entirely reasonable because of the O-H distance in water.

High temperature and/or high pressure water. We can assess the extent by which temperature and/or pressure influences the structure of water through examination of how the correlation functions vary as these two state variables are either raised or lowered. Qualitatively one can expect that as we lower temperature, structural order will increase as exemplified by results obtained on supercooled water (e.g., Dore et al. 2000; Botti et al. 2002). Conversely as we raise temperature we can anticipate a loss in ordering which will be reflected in a broadening of the various correlation peaks as well as some shift in peak positions. The changes in the structure of the three-dimensional hydrogen-bonded network of water are interrogated relative to the reference ambient temperature liquid using NDIS as described above.

At normal pressure, the structure of liquid water is fragile as manifested by its unusually large temperature dependence. Numerous neutron and X-ray scattering studies indicate that when water is isothermally compressed, the number of hydrogen bonds per water molecule is not altered by any appreciable amount relative to what is observed at ambient conditions (e.g., Bellissent-Funel and Bosio 1995; Yamanaka et al. 1994; Gorbaty and Demianets 1983; Gorbaty and Okhulkov 1994). However, the hydrogen bonds do become bent out of their ideal orientation and are correspondingly weaker energetically (Head-Gordon and Hura 2002). The most significant effects occur in the change of O-O separation with increasing pressure (into the 100's of MPa range) where the second peak in the $g_{OO}(r)$, indicative of local tetrahedral structure, is diminished with increasing pressure. With increasing pressure, the effect of temperature on liquid structure becomes smaller until the pressure dependency is nearly independent of temperature variation.

This is not the case when water is heated above ambient conditions up to and beyond the supercritical state points. By way of example we show the results of Soper et al. (1997) who provided a reassessment of both old and new diffraction data leading to improved site-site pair correlation functions of water from 25 to 400 °C and pressures up to 280 MPa (Fig. 3a-c). This composite plot (with the intramolecular portions removed) shows the changes in $g_{HH}(r)$, $g_{OH}(r)$, and $g_{OO}(r)$ as a function of increasing temperature and decreasing density. Despite some difficulties with small residual oscillations in these functions arising from non-trivial truncation and statistical uncertainties, qualitative trends are apparent. In the case of the O-H correlations (Fig. 3a) the first peak becomes significantly broader as the critical conditions are approached and appears to shift to larger radius values—i.e., from 1.85 Å at ambient conditions to about 2.15 Å at 573 K on the coexistence curve. The number of hydrogen bonds tends to decrease from 3.3 at ambient conditions to values more on the order of 2.2-2.4 at 573 K based on integration under the first O-H peak. In the supercritical state, at 673 K, this O-H peak no longer appears as a distinct peak and has been washed out into a broad shoulder. Based on these results it can be concluded that above the critical point, the hydrogen bonding in water has been significantly modified to the point where no distinct O-H site-site correlation peak is preserved. From an examination of the O-O correlation functions (Fig. 3b), we observe a similar trend wherein there is a gradual shift of the first peak to larger radius values with increasing temperature to a value of about 3.1 Å (X-ray diffraction data show this peak position to be closer to 3.5 Å). As temperature is increased to the critical point, the H-H pair correlations (Fig. 3c) exhibit a decided degradation of the pattern with considerable shoulder development even at 423 K to such an extent that it is difficult to tell how much the first ambient peak at 2.4 Å shifts with increasing temperature.

There can be no doubt that based on both neutron and X-ray diffraction, the molecular arrangement of water molecules is greatly perturbed at elevated temperatures compared to ambient water. The question that has been hotly debated in the past is whether or not there is

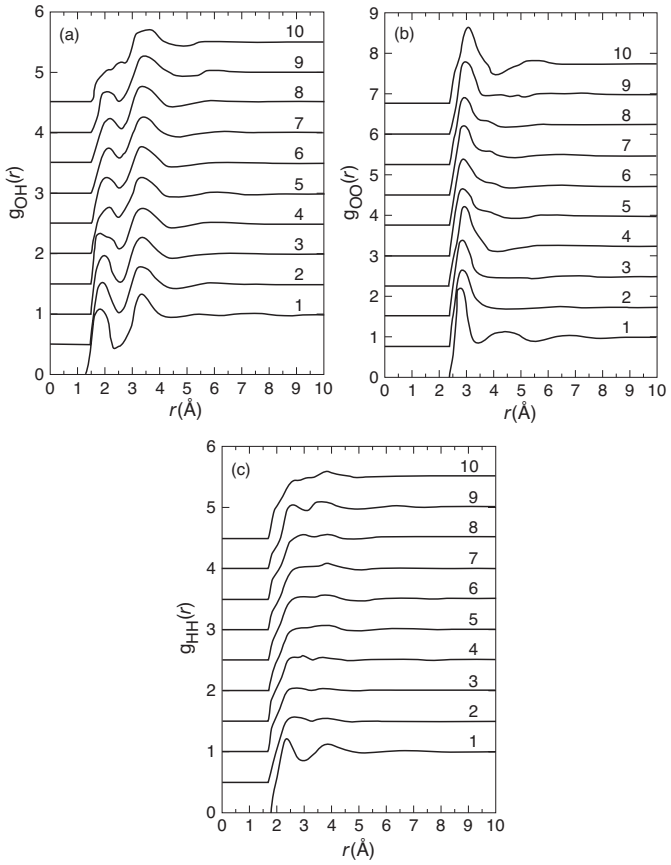

Figure 3. Radial distribution functions for H_2O: (a) $g_{OH}(r)$, (b) $g_{OO}(r)$ and (c) $g_{HH}(r)$ as a function of temperature and density from NDIS experiments. Temperature-pressure-density conditions: 1: 298 K, 0.1 MPa, 0.0334 molecules/Å^3; 2: 423 K, 190 MPa; 0.0334; 3: 423 K, 100 MPa, 0.0308; 4: 573 K, 280 MPa, 0.308; 5: 573 K, 197 MPa, 0.0296; 6: 573 K, 110 MPa, 0.0278; 7: 573 K, 5.0 MPa, 0.0260, 8: 573, 10 MPa, 0.0240; 9: 573 K, 9.5 MPa, 0.0240; 10: 673 K, 80 MPa, 0.0211. [Used by permission of the American Physical Society, from Soper et al. (1997), J Chem Phys, Vol. 106, Figs. 2, 3, 4, p. 251]

a temperature at or above which there is total breakdown of hydrogen bonding. According to the work of Soper et al. (1997) highlighted above, calculated bond angle distributions tend to suggest that the degree of true hydrogen bonding is greatly reduced in the supercritical state compared to ambient conditions. Complementary experimental studies using Raman (Walrafen et al. 1999), X-ray scattering (Gorbaty and Kalinichev 1995) and IR (Bondarenko and Gorbaty 1973) suggest that tetrahedral hydrogen bonding persists to at least 650 K and perhaps even up to 700 K at 100 MPa (Head-Gordon and Hura 2002). Bolstered by simulation studies using improved water models in concert with various scattering data, a consensus has been established that local hydrogen bonding is still present near the critical temperature and density, but that the space-filled percolating hydrogen-bonded network dominant at ambient conditions collapses.

Structure of aqueous solutions of geochemical relevance

Understanding the speciation of solutes (e.g., cations, anions, non-polar species, etc.) in aqueous solutions is a critical issue with direct impact on important geochemical processes such

mineral solubilities, metal mobilization and transport, and precipitation of potential contaminant phases. Of particular importance is the nature of ion hydration, rates of exchange of coordinated ions with water, and interaction energies between ions and water molecules. Given the current state of molecular-based experimental and modeling techniques, many of these aspects of complex aqueous solutions have been largely speculative and commonly model-dependent. The effect of dissolved ions on the average structure of water may range from negligible in very dilute solution to significant in concentrated solutions. The structure of water in aqueous solutions has commonly been described relative to the structure of pure water and terms such as "structure maker and "structure breaker" are intended to indicate deviations from the pure liquid (Soper and Turner 1993). These terms originated from the comparison of the correlation times of water molecules in aqueous solution with those in pure water (Ohtaki and Radnai 1993). Early on it was recognized that rather than focusing on single parameters such as the hydration number, the bond length, or the diffusion coefficient, that what really mattered were correlation functions which reflected the disordered and dynamic nature of aqueous solutions (e.g., Enderby 1983, 1995; Neilson and Enderby 1989).

In the context of an aqueous solution, let's revisit the concept of the radial distribution function, $g_{\alpha\beta}(r)$ related to the static structure. The function measures the probability of finding a β-particle at a distance r from an α-type particle placed at the origin. The average number of β-type particles that occupy a spherical shell of radius r and thickness dr at the same instance of time is given by:

$$dn_{\alpha\beta} = 4\pi\rho_{\beta}g_{\alpha\beta}(r)r^2dr \tag{16}$$

where $\rho_{\beta}= N_{\beta}/V$ and N_{β} is the number of β species contained in the sample of volume, V (Neilson and Enderby 1996). The integrated form of this expression was given in Equation (15). A multicomponent solution in the form of a salt (MX_n) in H_2O can be described by 10 pair radial distribution functions grouped into three sub-systems: three representing the solvent structure, $g_{HH}(r)$, $g_{OH}(r)$, and $g_{OO}(r)$; three characterizing the solute structure, $g_{MM}(r)$, $g_{MX}(r)$, and $g_{XX}(r)$; and four which describe the solute-solvent structure (hydration phenomena), $g_{MO}(r)$, $g_{MH}(r)$, $g_{XO}(r)$, and $g_{XH}(r)$. The difficulty is that a single diffraction pattern contains a weighted average of all 10 partial structure factors, and to disentangle them is far from trivial. To fully appreciate this complexity, refer to Equation (10) in Wilding and Benmore (2006, this volume) which describes the formalism for the total pair distribution function, $G_{\alpha\beta}(r)$.

In Figure 4a we show examples of two typical $g(r)$s which represent (a) $g_{MO}(r)$ and (b) $g_{MH}(r)$ for an aqueous solution. The ratio Δ/Δ' gives a measure of the stability of the aqua-ion hydration complex. From measurements of r_{MO} and r_{XO} and knowledge of the interatomic distances of the H_2O molecule, it is possible to determine the ion-water conformation and to calculate an average tilt, as depicted in Figure 4c. In principle by comparison of n_{MO} and n_{MH} one can evaluate the extent to which an aqua ion is acidic, since the dissociation given as:

$$[M(H_2O)_n]^{p+} = [MH_2O)_{n-1}(OH)]^{(p-1)+} + H^+ \tag{17}$$

will lead to $n_{MH} < 2n_{MO}$. In practice, however, only strong acid behavior (e.g., Fe^{3+}) has been detected because of the errors in determination of n (Neilson et al. 1993).

The difference methods of NDIS referred to above (and in Wilding and Benmore 2006, this volume) are ideally suited to the determination of structure in terms of the individual $g_{\alpha\beta}(r)$ or as their linear combinations of the form $G_{\alpha\beta}(r)$, which is specific to the isotopically substituted species α. The *first-order difference* method applied to cations or anions by isotopic exchange M^* for M or X^* for X can be used to obtain information concerning aqua-ion structure in terms of the function $G_M(r)$ or $G_X(r)$. For $G_M(r)$ we can show (from Enderby et al. 1987):

$$G_M(r) = A[g_{MO}(r) - 1] + B[g_{MH}(r) - 1] + C[g_{MX}(r) - 1] + D[g_{MM}(r) - 1] \tag{18}$$

where $A = 2c_Mc_Ob_O\Delta b_M$, $B = 2c_Mc_Hb_H\Delta b_M$, $C = 2c_Mc_Xb_X\Delta b_M$, $D = c^2{}_M(b^2{}_M - (b^*{}_M)^2)$, $\Delta b_M =$

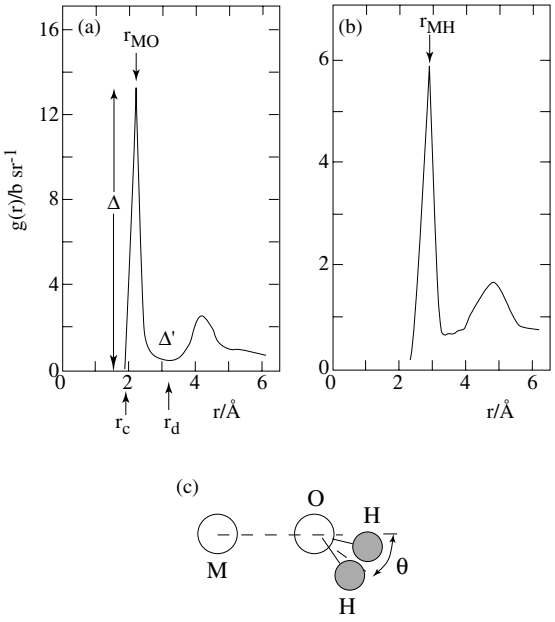

Figure 4. Two typical $g(r)$'s which represent (a) $g_{MO}(r)$ and (b) $g_{MH}(r)$ for a solution MX_n in H_2O. Δ/Δ' gives an estimate of the stability of the aqua-ion hydration complex. r_c is the nearest distance of approach of the two particles, r_{MO} and r_{MH} are the most probable nearest-neighbor separations between particles, r_d is the probable end of the first coordination shell. (c) Possible ion-water conformation and tilt angle, θ. [Used by permission of The Royal Society of Chemistry, from Neilson et al. (1993), J Chem Soc Faraday Trans, Vol. 89, Fig. 1, p. 2928]

$b_M - b_{M^*}$, and c is the atomic concentration of either M, X, O, or H (D), whose neutron coherent scattering length is b_i. In practice only the first two terms matter because c_M and $c_X << c_H$ and c_O such that the $G_M(r)$ reflects almost totally the structure of the coordination complex. The strength of the interactions dictate to a large extent the range of concentrations used in scattering experiments and in many cases molal quantities are required to achieve satisfactory results. Of course the key prerequisite here is having M cations (e.g., Li^+, K^+, Mg^{2+}, Ca^{2+}, Ni^{2+}, Zn^{2+}, Sr^{2+}, etc.) and X anions (Cl^-, I^-, NO_3^-, etc.) with isotopes exhibiting sufficient differences in their coherent scattering length (refer to Table 1 for a partial list). From our discussion of NDIS in water we know that H-D exchange occurs in all aqueous solutions such that by measuring the $G_M(r)$ for both heavy and light water, the $g_{MO}(r)$ and $g_{MH}(r)$ can be determined separately. This assumes that H and D can be treated as isomorphic—i.e., $g_{MH}(r) = g_{MD}(r)$. In an analogous manner, the hydration of anions can be studied, the derived quantities being, $G_X(r)$, $g_{XH}(r)$ [$= g_{XD}(r)$], and $g_{XO}(r)$. D_2O was used in the early applications of NDIS to salt solutions to avoid problems that could arise from the large incoherent scattering of H_2O. However, improvements in scattering technology made it possible to also work with salt solutions in H_2O.

The *second-order difference* experiments involving isotopic exchanges of M^* for M, X^* for X, and deuterium (D) for hydrogen (H) can be used to obtain individual pair functions for the solute [$g_{MM}(r)$, $g_{MX}(r)$, $g_{XX}(r)$] and the solvent [$g_{HH}(r)$, $g^*_{OH}(r)$]. Here the asterisk on $g_{OH}(r)$ denotes that it is only an approximation to the true $g_{OH}(r)$, except in the limit of greatly increased dilution where it will approach the exact function, as in pure H_2O. This approach makes it possible to improve resolution of ionic hydration structure especially with regard to the second hydration shell. It is worth repeating that because the scattering length of the oxygen isotopes, ^{16}O, ^{17}O, and ^{18}O, are almost identical, determination of $g_{OO}(r)$ in pure water is subject to large uncertainties, and is not readily accessible in solution. For a determination of either $G_M(r)$ or $G_X(r)$, it is preferential to work with solutions of heavy water, D_2O, because of the large incoherent scattering of the proton (H) spins and the large inelastic scattering of

the proton nuclei in H_2O. For the most part it is sufficient to only describe the total distribution, $G_M(r)$ or $G_X(r)$ unless one really needs to resolve the hydration at the pair distribution function level (Neilson et al., 2001). The hydration number, n_I for an ion, M or X, in solution can be defined from Equation 15 where the $g(r)$'s can be $g_{MO}(r)$, $g_{MH}(r)$, $g_{XO}(r)$, or $g_{XH}(r)$, and concentration of O as c_O or H as c_H appear outside the integral.

Rather complete reviews on complex solutions including aqueous electrolytes of interest to geochemists studied by neutron and/or X-ray scattering have been provided by Enderby (1995), Neilson and Adya (1997) and Neilson et al. (2002) so we will only highlight some relevant results to illustrate the power of neutron scattering.

Solvent structure. How the radial distribution functions of water change with an added salt are of considerable interest to geochemists. Manifestations of changes in water structure on the dissolution of ions are evident in many macroscopic experiments, e.g., changes in compressibility, solvation enthalpies and entropies, etc. H/D isotopic substitution of the water molecules in concentrated aqueous solutions (e.g., common chloride salts of LiCl, KCl, NaCl, etc.) is used to calculate $g_{HH}(r)$ and $g_{OH}(r)$, and estimate $g_{OO}(r)$, whose accuracy is appreciably less than the other two functions. For example, the increase in concentration of LiCl on $g_{HH}(r)$ is shown in Figure 5 for two solutions, 1 and 10 molal (mol/kg H_2O), compared against pure H_2O (Tromp et al. 1992). They concluded that both the intermolecular and intramolecular structure of water are relatively unaffected by the presence of salt at the 1 molal level. Clearly, at higher concentrations, a significant effect takes place, and in this case, at 10 molal, the number of hydrogen bonds decreases by about 30% from that characteristically of pure H_2O. This type of work was extended by Leberman and Soper (1995) to include other salts, NaCl, Na_2SO_4, and NH_4SO_4, and also more recently by Bruni et al. (2001), who examined effects of high concentrations (to 10 molar) of hydroxide, as NaOH, on water structure. Leberman and Soper (1995) concluded that ions effectively produce a change in water structure that is equivalent to an increase in pressure—i.e., ionic concentrations of a few molal have equivalent pressures that exceed 100 MPa. This is not entirely correct since pressure on a solution is isotropic whereas this effect is "localized" and solvent-mediated due to electrostriction about the ions. Interestingly, cations commonly found in nature, such as Na^+ and K^+, as chlorides, will also not significantly alter the structural properties of water solvent at concentrations less than about the 1 molal range (Horita and Cole 2004).

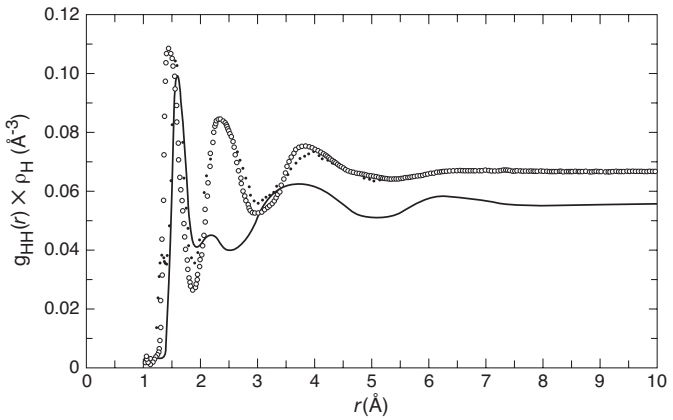

Figure 5. Partial pair radial distribution function $g_{HH}(r)$ multiplied by ρ_H; pure water – open symbols; 1 molal LiCl – dots; 10 molal LiCl – solid curve. [Used by permission of the American Physical Society, Tromp et al. (1992), J Chem Phys, Vol. 96, Fig. 7, p. 8467]

Ion-water structure. A tremendous amount of effort has gone into studies of ion-water interactions in aqueous solution. As noted above, recent reviews by Neilson and Adya (1997), Neilson et al. (2002), and most recently by Danielewicz-Ferchmin and Ferchmin (2004) provide very nice overviews on behavior of a wide range of cation and anion hydration behavior as interrogated by neutron, X-ray and computational methods. The NDIS method has contributed to the several key questions that are central to understanding this behavior including; (i) what are the length scales over which the primary hydration shell, secondary shell, intermediate zone and transition to bulk water range?; (ii) how sharply differentiated are these zones?; and (iii) how stable is the inner most hydration shell to changes in temperature, pressure, ion concentration and counter ion? We will only touch upon a few examples here to highlight how neutron scattering has contributed to answering these questions.

The alkali and alkaline earth metal ions (Li^+, Na^+ [isomorphic with Ag^+], K^+, Rb^+, Mg^{2+}, Ca^{2+}, Sr^{2+}) have probably been the most extensively studied of all the cations (e.g., Howell et al. 1991; de Jong and Neilson 1996, 1997). Example diffraction patterns, as $G_M(r)$ vs. r are shown in Figure 6. In general, as the ion size increases and the charge density is reduced there is a progressive weakening in the ion-water structure—i.e., the hydration shell becomes less well resolved. For example, the ionic hydration of Li^+ and Mg^{2+} (which is isomorphic with Ni^{2+}) is more clearly defined compare to that for K^+ or Sr^{2+}, respectively, and Na^+ and Ca^{2+} occupy

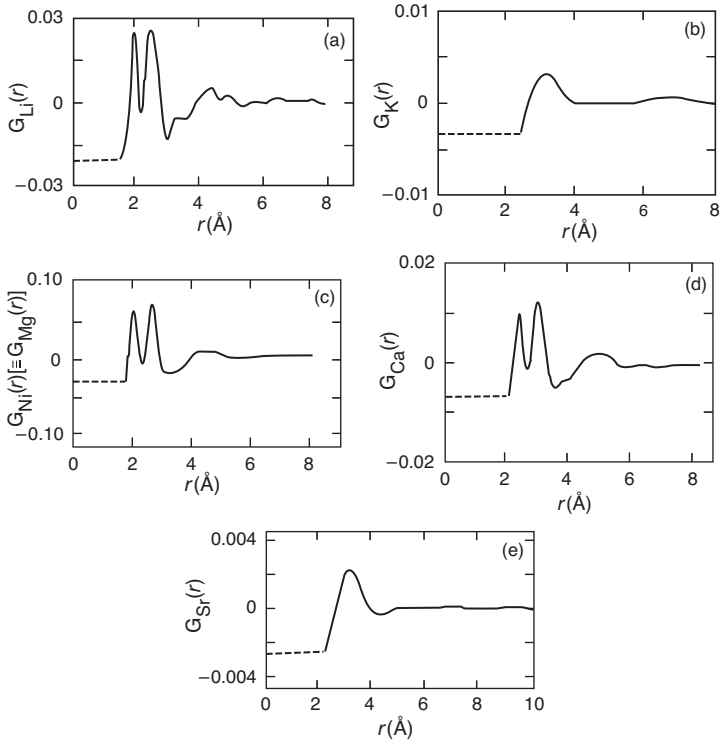

Figure 6. Examples of cation radial distribution functions $G_M(r)$ at 25 °C for (a) Li^+ in 3.6 M D_2O solution (Newsome et al. 1980); (b) K^+ in 4 M KCl D_2O solution (Neilson and Skipper 1985); (c) Ni^{2+} in a 2 M $NiCl_2$ D_2O solution (Powell et al. 1989), which is isomorphic with $MgCl_2$ in aqueous solution (Skipper et al. 1989); (d) Ca^{2+} in a 2.8 M $CaCl_2$ D_2O solution (Hewish et al. 1982); and (e) Sr^{2+} in a 3 M $Sr(ClO_4)_2$ D_2O solution (Neilson and Broadbent 1990). [Used by permission of Elsevier Ltd, Howell et al. (1991), J Molec Struct, Vol. 250, Figs. 2, 3, p. 286]

intermediate ion-water conformational structures. In particular, Sr^{2+} has a relatively weak hydration shell and no longer-range structure. Interestingly, it appears that the coordination number for the +1 valence alkali cations does not change appreciably from a value of between 5 and 7. As studies have shown that with the exception of Li^+, the extent of the perturbation to the structure of water is limited primarily to the range of the first hydration shell for alkali ions.

Other ions of interest to geochemists that have received considerable attention include transition metals (e.g., Cr^{3+}, Fe^{2+}, Fe^{3+}, Ni^{2+} and Cu^{2+}) and the lanthanides (Nd^{3+}, Dy^{3+}, Yb^{3+}). Characteristically, the transition metals have a first hydration shell usually containing 6 water molecules, a distinguishing second hydration shell, and considerable short-range ordering of water around them (Neilson et al. 2001). Of the transition metals, the most extensive work on aqua ion structure has been carried out on Ni^{2+} using NDIS, and is commonly used as a reference system to test the accuracy of other methods. This is particularly true when exploring the effects of increased concentration, temperature and pressure. NDIS experiments on aqueous solutions have been conducted at temperatures and pressures up to and beyond their critical points. It has been documented that the hydration structures of Li^+, Ni^{2+} and Cl^- are highly susceptible to changes in temperature, and there is a general reduction in hydration number with temperature presumably accompanied by an increase in anion-cation contact (Neilson and Adya 1997). Recently, Badyal and Simonson (2003) interrogated the effects of temperature (90, 175, 230 °C) on the hydration structure around Ni^{2+} in concentrated chloride solutions. They observed a gradual weakening of the hydration structure and a steady reduction in the average water coordination number with increasing temperature. Structural properties of the lanthanides have been less well investigated, but NDIS–based studies have suggested that the hydration number decreases approximately one unit across this series, from 9 to about 8 (e.g., Hahn et al. 1986; Helm et al. 1994; David et al. 2001).

The NDIS method has been used to interrogate the hydration behavior of important anions (Cl^-, Br^-, NO_3^-, ClO_4^-, etc.) but is particularly well suited to the study of chloride because of its favorable isotopes, ^{35}Cl and ^{37}Cl. It is considered as an ideal probe of structural perturbations which are induced when aqueous electrolyte solutions contain large polyions (Wilson et al. 1997; Tromp and Neilson 1996). In general, anion hydration is weaker than that for cations particularly for complex anions where the low charge density inhibits the formation of long-lived aqua-ion species (Herdman and Neilson 1990). Figure 7 shows example results (Botti et al. 2004) based on the *second-order difference* method for $g_{ClO}(r)$, $g_{ClH}(r)$ and $g_{ClCl}(r)$ for HCl (1:9 solution of HCl in H_2O at 298 K). The pronounced first peak in $g_{ClOw}(r)$ and $g_{ClHw}(r)$, along with a low first minimum indicate a well-defined first solvation shell and suggests that the Cl^- ions are likely substituting a water molecule in the H-bond network. There are 4.4±1.4 water molecules around each Cl^- ion with a radius of 3.5 Å from a central negative ion. Its structure is remarkably independent of counterion, concentration changes to ~1 molal, and moderate changes in temperature and pressure (Powell et al. 1993). At elevated concentrations above 1 molal, and in the presence of counterions such as Zn^{2+} or Cu^{2+}, there is an appreciable decrease in the coordination number from 6 to about 4. However, the general conformation of the $Cl - H_2O$ interaction does not change with concentration. The absence of a conformational change with concentration in nickel chloride solutions is probably the result of effective self-screening by the relatively strong Ni^{2+} cation (e.g., Tromp and Neilson 1996). The effect of temperature on Cl^- hydration appears to be more pronounced for relatively weaker counterions such as in LiCl solutions where the hydration shell is more strongly affected when compared to a solution such as $NiCl_2$.

Solute structure. Neilson et al. (2002) point out that determination of the pair radial correlation functions among ions in solution (e.g., Ni-Ni, Cl-Cl, Ni-Cl) represents one of the most challenging experimental aspects of the molecular-level characterization of aqueous solutions. *Second-order difference* experiments have been conducted at very high concentrations of LiCl (Ansell and Neilson 2000), copper chloride (Ansell et al. 1995), and nickel chloride and nickel sulfate (Howell and Neilson 1997). However, results from these

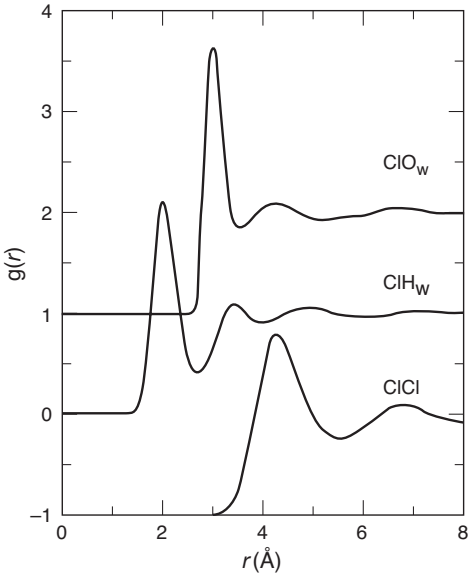

Figure 7. Radial distribution functions for $g_{ClHw}(r)$, $g_{ClOw}(r)$ and $g_{ClCl}(r)$ for HCl_{aq} at 298 K conditions (from Botti et al. 2004) around a central chlorine ion. The $g_{ClOw}(r)$ and $g_{ClCl}(r)$ have been shifted vertically for clarity. [Used by permission of the American Physical Society, Botti et al. (2004), J Chem Phys, Vol. 121, Figs. 3, p. 7843]

studies are not conclusive due to the difficulties inherent with this type of NDIS experiment. Enhancements in neutron intensity and instrument stability at facilities such as SNS offer the potential for more definitive *second-order difference* experiments on solute structure.

Dynamics in water and electrolyte solutions

Thus far we have restricted our discussion on bulk solutions to the structural aspects and have not addressed molecular dynamics behavior. Of particular interest are microscopic dynamical properties such as translation and rotation, diffusion, and the lifetime of hydrogen bonding in both pure water as well as aqueous solutions. At the microscopic level, liquid water may be viewed as a "transient gel" or a network of hydrogen bonds with a local tetrahedral symmetry. This picture was originally developed from the percolation model of Stanley and Teixeira (1980) and the connectivity properties have since been predicted by molecular dynamics (MD) simulations (e.g., Kalinichev 2001). It appears that the hydrogen bonded network includes small spatially-correlated "clusters" of four-bonded molecules and that the local density near a "cluster" is lower than the global density. The dimensions of the clusters have been evaluated by estimating their radius of gyration. The value of the mean characteristic length is approximately 20 Å whereas the correlation length of the density fluctuation has been measured by both X-ray (Michielsen et al. 1988) and neutron scattering (Bosio et al. 1989). It turns out that because of the differences between scattering cross sections of H_2O and D_2O, inelastic neutron scattering is a useful tool to probe the individual and collective motions of liquid water and water containing dissolved ions. Specifically, the diffusive motions (translation and rotation) can be interrogated by quasi-elastic neutron scattering (QENS), whereas the vibrational density of states, including both the inter- and intra-molecular parts, are accessible through the use of inelastic neutron scattering (INS). Many of these properties are strongly dependent on both temperature and pressure. The theoretical background for these two approaches is presented later in this chapter in the sections of fluid confinement and fluid-surface interactions, and to a limited extent in Loong (2006, this volume).

QENS is generally applied to the study of nonpropagating relaxation modes in liquids (e.g., Chen and Teixearia 1986). When applied to molecules containing hydrogen atoms, it mea-

sures the dominant incoherent scattering from them. In this case, the spectra are dominated by the Fourier transform of the van Hove self-correlation function of the H atoms. In liquid H_2O, the principle contributions to the quasi-elastic line are from the self-diffusion of the two equivalent H atoms and from the short-time reorientation of the molecule. QENS studies have been conducted on water (as either H_2O or D_2O) at ambient to supercooled conditions (e.g., Chen et al. 1982, 1999; Teixeira et al. 1985; Bellissent-Funel and Teixeira 1991; Petrillo et al. 2000), in the supercritical range (e.g., Tassaing and Bellissent-Funel 2000; Uffindell et al. 2000; Beta et al. 2003), and at high pressure (Cunsolo et al. 2006). Parameters obtained from QENS include the residence time, τ_o (in ps) which has the strongest temperature dependence, a reorientational (hindered rotation) time, τ_1 (in ps), which exhibits Arrhenius behavior (E_A = 1.85 kcal mol^{-1}), and the characteristic mean jump diffusion length, L in Å. As seen in Figure 11 below (Confinement section), both τ values increase with decreasing temperature, with τ_o displaying a relative steep non-linear slope (1.25 ps at 20 °C to >10 ps at −20 °C). We know that water molecules are instantaneously connected with most of their neighbors through hydrogen bonds. The breaking of hydrogen bonds is due to the libration motions which have large amplitudes and occur when the vibrational angle exceeds the critical value of 28°. When at least three bonds are broken simultaneously diffusion is possible where the proton jumps to the nearest site which is at an average distance L of about 1.6 Å. The value τ_o is a direct measure of the average duration which is required for a water molecule to break loose from its hydrogen bondage by rotational excitation. The τ_o is a time constant that no other technique except neutron scattering can access. The time associated with hindered rotations defined by τ_1 is interpreted as the typical hydrogen-bond lifetime. Because the number of hydrogen bonds increases with decreasing temperature, the diffusion process is strongly temperature dependent. At supercritical conditions for water (400-450 °C), τ_o remains relatively constant at 0.29-0.3 ps. The self-diffusion coefficient increases significantly with increasing temperature and decreasing density with values of 3.71-5.21 × 10^{-4} cm^2 s^{-1} for the T interval of 400-450 °C (Beta et al. 2003). Based on QENS results, it appears that even at supercritical conditions, motion in water is still constrained by the presence of a non-trivial degree of hydrogen bonding.

QENS has also provided the means by which ions (cations in particular) can be characterized according to the lifetimes of water molecules in cationic hydration structures on time scales of the order of 10^{-9} sec—i.e., smaller than those accessible by nuclear magnetic relaxation techniques where the lowest limit is ~10^{-7} s (e.g., Herdman and Neilson 1990). The QENS method allows one to differentiate between those cations which hydrate water molecules on timescales, τ_b much longer than 5×10^{-9} s or much shorter than 10^{-10} s; it is also possible to identify cations such as Cu^{2+} and Zn^{2+} with hydration shells which exchange water molecules with the bulk on a timescale of $5 \times 10^{-9} \geq \tau_b / s \geq 10^{-10}$. Figure 8 summarizes the residence times of water molecules in the neighborhood of aqua ions and ranges of experimental techniques that be used to interrogate specific timescales (Neilson and Enderby 1989). For a more complete, although not very recent summary of the translational self-diffusion coefficients for ions, residence times of water in the first hydration shell, reorientational time of hydrated water molecules, and rates of water substitution reactions involving ions, refer to the nice compendium provided by Ohtaki and Radnai (1993). Inspection of Figure 8 indicates that ions (usually strong cations such as Ni^{2+} or Cr^{2+}) which can coordinate with protons for a time >5×10^{-9} s are said to possess hydrated water molecules that exchange slowly with the bulk water. Conversely, water molecules coordinated to weak cations (e.g., Na^+, Li^+, Cs^+) and all anions (e.g., Cl^-, I^-, F^-) exchange with bulk water on a timescale <10^{-10} s which is classified as fast exchange. There are also several cations with hydrated water molecules which exchange with bulk water in an intermediate time domain of ~10^{-9} s such as some of the lanthanide cations.

Role of molecular-based simulations in neutron diffraction studies

A comparison between experimental scattering data and simulations lies at the heart of the validation of any molecular-based modeling effort. In recent years there has been a

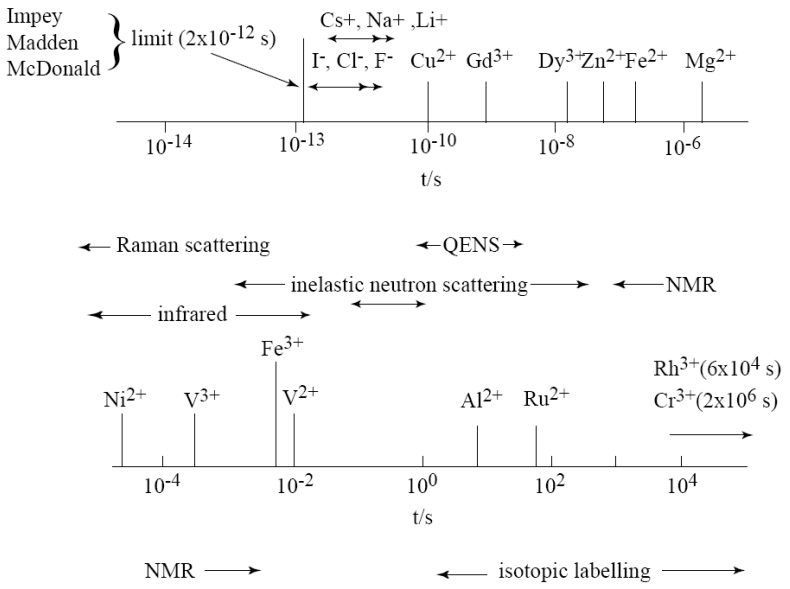

Figure 8. Residence times of water molecules in the neighborhood of aqua ions, and ranges of experimental techniques available to interrogate these time scales. [Used by permission of Elsevier Ltd., from Neilson and Enderby (1989), Adv Inorg Chem, Vol. 34, Fig. 2, p. 197]

constructive interplay between various types of simulation methodologies (e.g., reverse Monte Carlo, EPSR, classical and *ab initio* MD, density functional theory, etc.) and neutron scattering experiments over the full range of temperature and pressure, but particularly so on supercritical water (e.g., Soper 1996, 2005; Chialvo et al. 1998). A full discussion of this important component of neutron scattering studies is beyond the scope of this review, but a few comments are worth making that emphasize the importance of making the synergistic link between theory, modeling and simulation (TMS) and experimental results. For recent examples of these links, the reader is encouraged to examine the very nice summary provided by Kalinichev (2001) who described the molecular simulations of liquid and supercritical water, and Soper (2005) who presented in more detail the utility of the EPSR method. An interesting new result (Chialvo and Simonson 2006) demonstrates that MD simulation in concert with *first-order difference* experiments involving null and heavy water can be used to assess the magnitude of $M^{\nu+}$-$X^{\nu-}$ ion-pair formation for a salt $M^{\nu+}X_n{}^{\nu-}$ in aqueous solution.

It was recognized in the mid 1990's that existing potential models for water did not adequately predict the features of the partial pair distribution functions, $g(r)$ for water measured by neutron scattering (e.g., Chialvo and Cummings 1998). It was unclear whether the disagreement between predicted and measured correlation functions was a reflection of unrealistic intermolecular models, inadequate processing of the raw NDIS data, or a combination of both. Suspicion focused on the inadequacies in the proper accounting of the inelasticity (Placzek errors) corrections associated with the NDIS experiments. These corrections become a large source of uncertainty at high temperature and remarkably difficult to estimate for the light isotopes. Molecular models pinpointed the inaccuracies in the scattering data, while at the same time revealing that improvements in how to constrain the hard-core diameters used in models helped avoid unphysical behavior over short length scales (Chialvo et al. 1998). Several conclusions were reached that are important for future work on the molecular features of water: (a) There is incentive to build new neutron instruments that use 0.1 Å wavelengths to help minimize problems associated with the inelastic correction; (b)

There is a need for an independent method to verify NDIS data because of its experimental complexity and the likelihood of undesirable numerical artifacts in the raw data; (c) It would be desirable to develop alternative experimental methods to determine microstructure, to avoid use of isotopic substitution and its troublesome inelasticity correction; and (d) We need alternative or complementary molecular-based methods to efficiently check the reliability of experimental structural results, before they are used in model parameterization.

FLUIDS CONFINED IN NANOPOROUS REGIMES

Confining matrices of interest to earth sciences

The behavior of liquids in confinement typically differs from their bulk behavior in many ways. Some important factors influencing the structure and dynamics of confined liquids include the average pore size and pore size distribution, the degree of pore interconnection, and the character of the liquid-surface interaction (e.g., hydrophilic vs. hydrophobic pore surfaces). While confinement of liquids in hydrophobic matrices, such as carbon nanotubes, or near the surfaces of mixed character, such as many proteins, had been the area of rapidly growing interest, the confining matrices of interest to earth sciences usually contain oxide structural units and thus are characterized by hydrophilic pore surfaces. This is because, unless dehydroxylation procedures are applied, there is always chemisorbed water on an oxide surface in the form of hydroxyl groups. The pore size distribution and the degree of interconnection vary greatly amongst porous matrices. At one end of the spectrum there are materials with irregular porous structure, such as porous glasses (e.g., Vycor), xerogels, aerogels, and rocks. At the other end, there are materials characterized by regular porous structure, such as mesoporous silicas (e.g., SBA-15, MCM-41, MCM-48), zeolites, and layered systems, for instance, clays. In many matrices, the pore size may be tailored by means of adjusting the synthesis regimen. In clays, the interlayer distance may depend on the level of hydration. Although studied less frequently, matrices such as artificial opals and chrysotile asbestos represent other interesting examples of ordered porous structures. In this section, we provide a brief review of research performed on liquids confined in materials of interest to the earth sciences (silicas, aluminas, zeolites, clays, rocks, etc.) using various neutron scattering techniques with special emphasis on dynamical behavior.

Neutron scattering as a probe of confinement processes

The properties of neutrons make them an advantageous probe for studying liquids in confinement compared to X-rays. Neutrons can be scattered either coherently or incoherently, thus providing opportunity for various kinds of analysis of both structural and dynamic properties of confined liquids. Such analysis is possible due to the fact that wavelengths of thermal and cold neutrons are comparable with intermolecular distances in condensed phases, while the neutron energy can be tailored to probe both high- (collective and single-particle vibrational) and low-frequency (single-particle diffusive) motions in the system. Importantly, the large incoherent scattering cross-section of hydrogen compared to other elements allows acquisition of spectra dominated by the scattering from H-containing species (see recent review article by Neumann 2006), whereas the X-ray scattering from such systems, which is virtually insensitive to hydrogen, would be dominated by the signal from the confining matrix. Last but not least, the large difference in the coherent and incoherent neutron scattering cross-sections of hydrogen and deuterium allows preferential selection of atoms to dominate the scattering signal by means of selective deuteration of the fragments of liquid molecules or the confining matrix.

Application of various techniques: neutron diffraction, small-angle scattering, inelastic spectroscopy

The structural properties of confined liquids can be assessed using coherent scattering techniques, neutron diffraction and small-angle neutron scattering (SANS). The former allows

one to measure the static structure factor, $S(Q)$, which can be then Fourier-transformed to obtain the radial pair-distribution function, $g(r)$, that describes the distribution of the distances between the coherently scattering nuclei in the liquid. For hydrogen containing species, deuteration is required in order to obtain diffraction patterns from coherently scattering D nuclei.

Perhaps the most important application of neutron diffraction from confined liquids is detection of freezing-melting transitions. These transitions are known to be depressed to lower temperatures compared to the corresponding bulk liquids and to exhibit a substantial hysteresis. Unlike, for example, calorimetric measurements, a neutron diffraction experiment can not only detect a freezing transition in the confined liquid, but also determine the crystal structure of the resultant solid phase. This phase may be either crystalline but different from that of the bulk solid phase, or amorphous. Information on the average size of the crystalline particles in confinement can be obtained from broadening of the Bragg peaks.

Most of the neutron diffraction studies of freezing of the supercooled confined liquids involved water-ice transition in mesoporous silicas, silica sol-gels, or Vycor glass (e.g., Steytler et al. 1983; Bellissent-Funel et al. 1992; Takamuku et al. 1997; Baker et al. 1997; Dore et al. 2002; Venuti et al. 2004). A review by Dore covers a number of structural studies of supercooled confined water (Dore 2000). It was found by several researchers that in sufficiently small pores formation of a metastable cubic ice phase takes place instead of a bulk hexagonal ice phase. In even smaller pores, where the development of hydrogen-bonded network is strongly suppressed, formation of amorphous ice was observed. Even though the temperatures in experiments with supercooled confined water are outside the range which is typically of interest to earth sciences, such experiments are important because they elucidate the effect of confinement on hydrogen-bonded network. The structure of liquid water confined in Vycor glass at ambient temperature was also addressed (e.g., Bruni et al. 1998).

In general, studies involving porous silicas as confining matrices typically emphasize the nature of the hydrogen-bonded network of confined water molecules, whereas water-matrix interactions receive less attention. These interactions, however, are of central importance in another active area of structural studies that concerns liquid-like interlayer water in clays (e.g., Skipper et al. 1990, 1994, 1995; Williams et al. 1997, 1998; Powell et al. 1998; de Siqueira et al. 1999; Pitteloud et al. 2000, 2001, 2003). In these studies, H/D isotopic substitution was typically employed in order to separate the diffuse diffraction pattern due to interlayer water from the Bragg diffraction due to the crystalline structure of the clay. The emphasis in the clay experiments is usually on the interaction of water molecules with the inter-layer counterions and the hydration structure of these counterions. These experiments are typically carried out at room temperatures. We note in passing that the neutron diffraction technique in combination with standard methods of crystallographic analysis such as Rietveld structural refinement is well suited to address the structural position of D_2O or deuterated organic molecules adsorbed in structurally complex crystalline materials such as zeolites (e.g., Goyal et al. 2000; Floquet et al. 2004).

While diffraction measurements of liquids in confinement probe structural correlations not exceeding a few molecular diameters, SANS measurements provide coverage over much broader range in the real space (Radlinski 2006, this volume). This is because SANS involves measuring neutron intensities at very low values of the scattering vector, $\mathbf{Q}$ (i.e., at small angles). For a two-phase system, the SANS intensity is proportional to the scattering contrast, i.e., the square of the difference in the scattering length densities between the two phases. Therefore, information on both the magnitude and the spatial distribution of the scattering density variations can be obtained from SANS data. The molecular-level structure of the constituencies is unimportant because it is averaged out over large distances. This is exploited to a good advantage in contrast variation methods (e.g., deuteration of hydrogenous phases), when the pores are filled, or partially filled with an adsorbate to bring the difference in the

scattering length densities (and, concurrently, the SANS intensity) to zero. For instance, in a contrast variation experiment open and closed pores could be distinguished since the latter would be inaccessible to the adsorbate. The contrast technique can be used to study the structures of both the empty pores and the adsorbate. In general, these structures do not have to be the same, especially in matrices with fractal pores, since an adsorbate may condense in the most strongly curved pore regions rather than cover the surface with a wetting film of uniform thickness (e.g., capillary condensation, Broseta et al. 2001).

SANS provides considerable flexibility in the choice of an adsorbate because the scattering length density can be tuned through partial deuteration of the adsorbate molecules. For a reader interested in a brief introduction to the SANS technique as well as a survey of the experimental results the review paper by Ramsay (1998) can be recommended. Fluids in various confining environments have been studied by SANS. Examples include water in Vycor glass and other porous silicas (Li et al. 1994; Agamalian et al. 1997), water in a synthetic clay and a natural rock (Broseta et al. 2001; Knudsen et al. 2003), and binary mixtures in various porous matrices (Dierker and Wiltzius 1991; Lin et al. 1994; Frisken et al. 1995), to name a few. Investigation of the liquid-gas critical phenomena in single-component fluids in confinement is another interesting area of SANS research (e.g., studies of cyclohexane in porous silica by Webber et al. (1996) and of carbon dioxide in a silica aerogel by Melnichenko et al. (2004, 2005, 2006)). Typically, SANS experiments are carried out at ambient or elevated temperatures (usually a few tens of degrees).

Dynamics of confined liquids is investigated by neutron spectroscopy that relies mainly on the incoherent scattering of neutrons from hydrogen nuclei. Even though the actual motions of nuclei in the molecules of a condensed phase are very complex, they usually can be separated into fast vibrational and librational and slow rotational and translational motions. The more energetic vibrational and librational modes are probed using dedicated neutron spectrometers with moderate energy resolution and reasonably high incident neutron energies. On the time scale of such spectrometers, rotational and translational motions are very slow and can be neglected. This type of measurement is known as inelastic neutron spectroscopy (INS). Compared to infrared spectroscopy, INS benefits from the absence of optical selection rules and the large incoherent scattering cross-section of hydrogen.

As in the structural studies, water is the medium whose dynamics in confinement has been studied most extensively. Traditionally, the field was dominated by studies of water (or hydroxyl groups) dynamics in zeolites (e.g., Jobic et al. 1992, 1996; Mitchell et al. 1993; Beta et al. 2004; Corsaro et al. 2005). More recently, INS was used to probe dynamics of hydroxyl groups in mesoporous silica (Geidel et al. 2003). In such studies, the fundamental vibrational modes of water molecules and hydroxyl groups adsorbed at well defined sites of the host framework are usually probed at low (helium) temperatures with neutron energy loss in order to sharpen the inelastic peaks, which suffer loss in quality due to multiphonon scattering in ambient temperature measurements with neutron energy gain. It should be noted that measuring the high-frequency stretching modes of OH and H_2O species (with an energy is excess of 400 meV or 3200 cm^{-1}) with neutron energy loss requires an inelastic neutron spectrometer built either at a spallation neutron source or a hot reactor neutron source in order to have access to sufficiently high incident neutron energies. Another recent development in the area of INS studies of confined liquids concerned measuring low-frequency (at about 100 meV and below) dynamics in supercooled water confined in Gelsil and Vycor glasses (Venturini et al. 2001; Crupi et al. 2002a,d). The emphasis in this area of research is on the properties of confined water, as opposed to studies of zeolites, where measured vibrational frequencies are typically used to characterize the adsorption sites.

There have been numerous INS studies of molecules other than water adsorbed in zeolites; e.g., alcohols (Schenkel et al. 2004a,b), chloroform (Mellot et al. 1998; Davidson et al. 2000),

ethane and ethene (Henson et al. 2000), furan (Beta et al. 2001), ferrocene (Kemner et al. 2002), also see Jobic (1992, 2000b) for surveys of earlier and more recent zeolite studies. A study by Rosi et al. (2003) that has attracted much interest involved investigation of hydrogen adsorbed in metal organic framework MOF-5. The INS spectra indicated the presence of two well-defined binding sites in this material, which is characterized by significant hydrogen uptake. As in the case of confined water, INS studies of organic molecules in confining matrices with a well-defined structure are mainly aimed at characterization of the adsorption sites. A study of propylene glycol confined in a porous glass by Melnichenko et al. (1995) represents an example of research where the properties of the confined medium were of the main interest.

Basics of quasielastic neutron scattering (QENS)

Quasielastic neutron scattering (QENS) can be used to assess the mobility of confined liquids, which is the property affected the most by a confinement: a change by one to two orders of magnitude in the mobility of a confined liquid is common. Here we provide the most basic description of the technique; for a detailed discussion see Bée (1988), Roe (2000), and Hempelmann (2000).

The incoherent scattering function $S_{\text{inc}}(Q,E)$ measured in an experiment is the space and time Fourier-transform of the self-correlation function $G_{\text{self}}(r,t)$, which is the probability that a particle that was at $r = 0$ at $t = 0$ is at position r at time t:

$$S_{\text{inc}}(Q,E) = \int I_{inc}(Q,t) e^{i\frac{E}{\hbar}t} dt = \int\int (G_{self}(r,t) e^{-iQr} dr) e^{i\frac{E}{\hbar}t} dt \tag{19}$$

where the intermediate scattering function, $I_{\text{inc}}(Q,t)$, is the space Fourier transform of $G_{\text{self}}(r,t)$. For the simplest case of Fickian diffusion with a diffusion coefficient D:

$$G_{\text{self}}(r,t) = \frac{e^{\left(-\frac{r^2}{4Dt}\right)}}{(4\pi Dt)^{3/2}} \tag{20}$$

$$I_{\text{inc}}(Q,t) = e^{-tDQ^2} \tag{21}$$

$$S_{\text{inc}}(Q,E) = \frac{1}{\pi} \frac{\hbar DQ^2}{(\hbar DQ^2) + E^2} \tag{22}$$

That is, the signal measured by a spectrometer as a function of neutron energy transfer, E, is a Lorentzian with a half width at half maximum (HWHM) $\Gamma = \hbar DQ^2$. In general, QENS probes rotational and translational diffusive motions of molecules that result in the broadening of the elastic peak. In QENS measurements, the effects of faster vibrational and librational motions manifest themselves in the overall reduction of scattering intensities (Debye-Waller factor). It should be noted that knowledge of the resolution function and an extremely good energy resolution is of paramount importance in QENS. For this reason, time-of-flight and backscattering spectrometers built at cold neutron sources are frequently employed in this type of experiment. Though conceptually different from QENS, neutron spin-echo technique, which has very high energy resolution and yields the intermediate scattering function in the time space, $I(Q,t)$, can be also used for studying slow diffusive motions.

Diffusion in confined and bulk liquids cannot be completely described by Equations (20-22). A simple model that captures the essential features of the diffusion process is called the "jump diffusion" model. It assumes that the diffusing particles rest for a time τ_T between jumps at a distance r. In this model, the scattering function in the energy space is still a Lorentzian for a translational diffusion process, but the Q-dependence of its broadening becomes:

$$\Gamma(Q) = \frac{\hbar}{\tau_T}\left(1 - \frac{\sin(Qr)}{Qr}\right) \tag{23}$$

(Bée 1988). The residence time between jumps and the jump length are related through the diffusion coefficient $D = r^2/6\tau_T$. A fixed jump-length jump diffusion model describes translational diffusion of interstitial species in some solids. In liquids, which are characterized by a distribution of jump lengths, $P(r)$, the HWHM averaged over the jump lengths becomes:

$$\Gamma(Q) = \frac{\hbar}{\tau_T}\frac{\int_0^\infty \left(1 - \frac{\sin(Qr)}{Qr}\right)P(r)dr}{\int_0^\infty P(r)dr} \tag{24}$$

The choice of $P(r)$, which is not unique, defines the Q-dependence of the HWHM. Two models are typically employed. For a Gaussian distribution of jump lengths, the half width at half maximum derived by Hall and Ross (1981) is:

$$\Gamma(Q) = \frac{\hbar}{\tau_T}\left[1 - \exp(-DQ^2\tau_T)\right] \tag{25}$$

where the three-dimensional diffusion coefficient $D = \langle r^2\rangle/6\tau_T$. Alternatively, an exponential distribution of jump lengths (Singwi and Sjölander 1960; Egelstaff 1967) yields:

$$\Gamma(Q) = \frac{\hbar}{\tau_T}\left[1 - \frac{1}{1 + DQ^2\tau_T}\right] \tag{26}$$

For both types of distribution, $\Gamma(Q \to 0) = \hbar DQ^2$ and $\Gamma(Q \to \infty) = \hbar/\tau_T$. Therefore, for a translational diffusion process the residence time between jumps and the diffusion coefficient can be obtained from the high- and low-Q limits of the QENS broadening, respectively.

To simplify analysis, faster rotational and slower translational diffusion motions are usually assumed to be independent (decoupling approximation). Then in the time space one can write the intermediate scattering function as a product of the rotational and translational components. Consequently, the scattering function in the energy space becomes a convolution of the rotational and translational components. A number of model scattering functions describing various types of rotational or other localized motions are discussed by Bée (1988). A common feature, which distinguishes them from the translational scattering functions such as the one described by Equation (22), is the existence of an elastic term due to a finite probability of finding a diffusing particle at the initial position at time t. This elastic term is frequently called elastic incoherent structure factor (EISF). For a rotational diffusion process, both the characteristic time between rotational jumps and the jump geometry can be derived from the Q-dependences of QENS broadening and the EISF. Refer to the section on *Fluid Interaction with Surfaces* for a more detailed discussion of scattering functions characterizing rotational diffusive motion.

Application of QENS to fluid-confined systems

The landmark study of supercooled bulk water by Teixeira et al. (1985) has established the framework for interpretation of QENS data from bulk water and water in various confining matrices. Examples of the QENS spectra obtained from water at various values of Q are shown in Figure 9. The Q-dependence of the Lorentzian broadening describing the translational diffusion component is shown in Figure 10. Fits of good quality could be obtained for the data through the entire temperature range using Equation (26). In this study, the water had to be supercooled in order to separate characteristic times between the rotational and translational

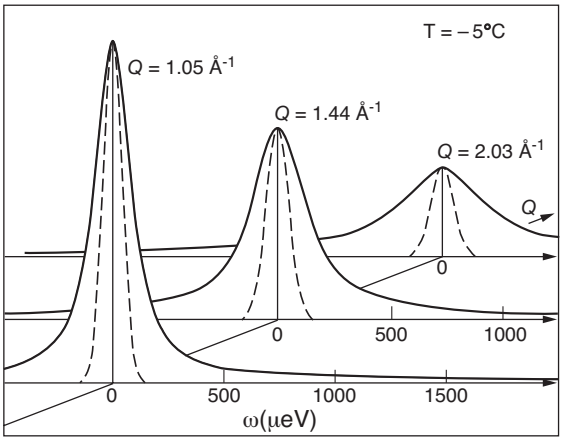

Figure 9. QENS data from supercooled water. [Reprinted with permission from Teixeira et al. (1985), Phys Rev A, Vol. 31, Fig. 1, p. 1915. © 1985 by the American Physical Society. URL: *http://link.aps.org/abstract/PRA/v31/p1913*]

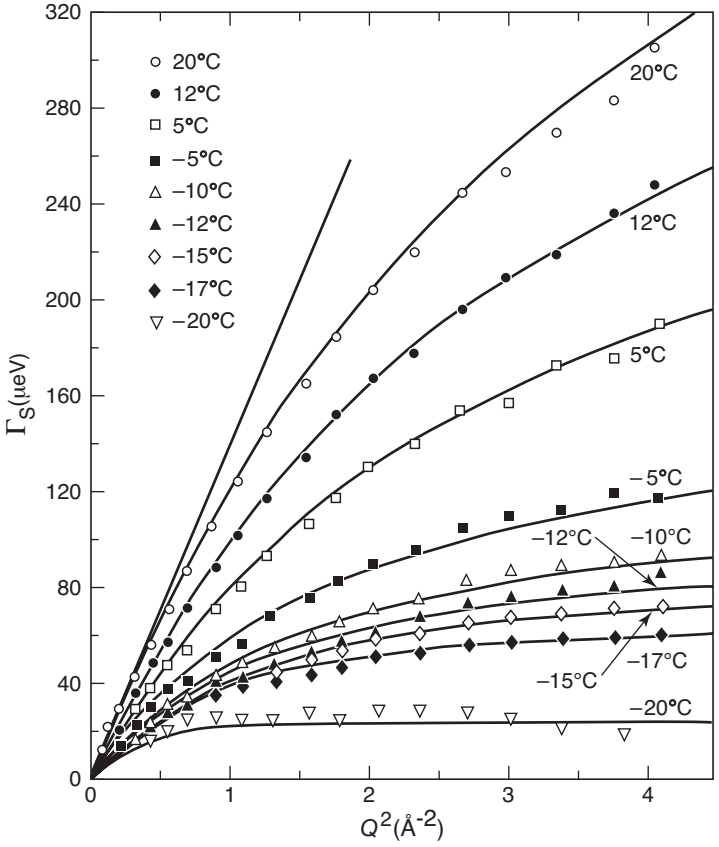

Figure 10. Linewidth of the translational diffusion component of supercooled water fitted with a model assuming exponential distribution of diffusion jump lengths. [Reprinted with permission from Teixeira et al. (1985), Phys Rev A, Vol. 31, Fig. 2, p. 1915. © 1985 by the American Physical Society. URL: *http://link.aps.org/abstract/PRA/v31/p1913*]

diffusion jumps. In bulk water, these characteristic times are both close to a picosecond at ambient temperature. Upon supercooling down to 253 K, the translational jumps slow down by an order of magnitude, whereas the time between rotational jumps increases by just about a factor of two, as one can see in Figure 11. Remarkably, confined water shares many of the same features observed in supercooled bulk water. In particular, the rotational diffusion jumps of water molecules in confinement tend to slow down much less compared to the translational diffusion jumps. Thus, the translational and rotational diffusion components are usually well separated at ambient temperature.

Because of the similarity between supercooled bulk and confined water, numerous studies of supercooled water in mesoporous silicas (Takamuku et al. 1997; Takahara et al. 1999; Mansour et al. 2002; Faraone et al. 2003b,c; Liu et al. 2004; Takahara et al. 2005), Vycor glass (Bellissent-Funel et al. 1993, 1995; Zanotti et al. 1999), and Gelsil glass (Crupi et al. 2002b,c) are relevant to understanding the mobility of water in confinement through a wide temperature range. As a result of these studies, two conceptually different approaches have evolved for interpretations of the QENS data on confined water. One is the "confined diffusion" model, where the shape and size of the confining pore manifest itself through the form-factor, which defines the Q-dependence of the EISF. This model assumes that water molecules perform unrestricted diffusion jumps within a pore until they encounter the pore boundaries. The second concept, commonly called "relaxing cage" model (Chen et al. 1995; Zanotti et al. 1999), suggests that on the time scale of translational jumps of a water molecule, the relevant confinement size is not the size of the pore, but that of the "cage" formed by the neighboring water molecules, from where the molecule can escape through the structural relaxation. In the

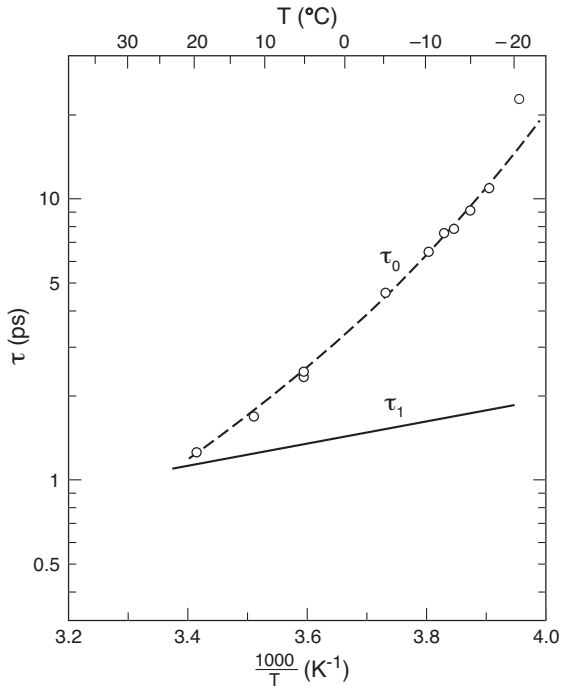

Figure 11. Temperature dependence of residence times for the translational (denoted τ_0) and rotational (denoted τ_1) diffusion components of supercooled water [Reprinted with permission from Teixeira et al. (1985), Phys Rev A, Vol. 31, Fig. 3, p. 1916. © 1985 by the American Physical Society. URL: *http://link.aps.org/abstract/PRA/v31/p1913*]

"relaxing cage" model, the self-correlation function is not a Gaussian, and the functional form of the intermediate scattering function in the time space is no longer described by the simple exponential decay as in Equation (21). Instead, it is represented by a stretched exponential decay, $\exp[-(t/\tau)^{\beta}]$. A stretched exponential decay has the same functional form one can obtain assuming a distribution of local diffusivities in the confined medium (Colmenero et al. 1999).

QENS studies of water confined in materials other than silica tend to focus on the influence of the matrix parameters (such as cation charge and channel size in zeolites) on the water dynamics. Various examples of matrices used to confine water include zeolites (Paoli et al. 2002; Crupi et al. 2004a,b,c), porous alumina (Mitra et al. 1998, 2001), tuff (Maddox et al. 2002), layered silicate AMH-3 (Nair et al. 2005), aluminosilicate glasses (Indris et al. 2005), and a silica-alumina-NaO_2 molecular sieve (Swenson et al. 2005). In these studies, ambient and elevated temperatures were of primary interest, even though it was possible to supercool water confined in small pores. In an interesting series of experiments, Fratini et al. (2001, 2002) and Faraone et al. (2002) investigated the dynamics of water in cements (hydrated dicalcium and tricalcium silicates) as a function of aging (i.e., cement curing time) at ambient temperature. Water mobility in clays is an actively developing area (e.g., Gay-Duchosal et al. 2000; Swenson et al. 2000; Swenson et al. 2001a,b; Malikova et al. 2005, 2006). Because oriented clay platelets are readily available, it is possible to differentiate between in-plane and out-of-plane interlayer water dynamics by means of properly orienting the sample with respect to the scattering vector. Both ambient and supercooled temperature regimes of interlayer water diffusion in clays have been investigated. Examples of the less common systems interrogated by QENS to study the dynamics of confined water include a layered material V_2O_5 (Takahara et al. 2000; Kittaka et al. 2005) and chrysotile asbestos ($Mg_3Si_2O_5(OH)_4$) fibers with macroscopically aligned one-dimensional channels (Mamontov et al. 2005b).

Mobility of confined materials other than water has been also investigated in a number of QENS studies. Examples include hydrogen (Glanville et al. 2003), methane (Benes et al. 2001), toluene (Alba-Simionesco et al. 2003), and cyclohexane (Jobic et al. 1995) in micro- and mesoporous silicas, *n*-hexane (Stepanov et al. 2003; Jobic et al. 2003), H_2/D_2 (Fu et al. 1999; Bär et al. 1999; Jobic et al. 1999), N_2 and CO_2 (Papadopoulos et al. 2004), benzene (Jobic et al. 2000b) and propane (Mitra and Mukhopadhyay 2003) in zeolites, and benzene in chrysotile asbestos fibers (Mamontov et al. 2005a). In these experiments, the temperature range varied greatly, depending on the properties of the confined material. It should be noted that the signal from coherently scattering nuclei is dependent on collective properties (such as transport diffusivity), whereas the signal from incoherently scattering nuclei such as H, which is measured in the overwhelming majority of QENS experiments, describes self-diffusion. While both QENS and neutron spin-echo techniques can measure data from coherently and incoherently scattering samples, spin-echo is intrinsically more effective for coherent scattering measurements. This is why most spin-echo measurements involve deuterated samples and probe transport rather than self-correlation properties. Studies by Swenson et al. (2001) and Jobic et al. (2000a) provide examples of spin-echo experiments on hydrogenated (water) and deuterated (benzene) liquids in confinement, respectively.

Dynamics of complex hydrocarbon molecules in confinement has been also addressed by QENS. Jobic (2000a) studied linear and branched alkanes (for chains up to C-14) confined in ZSM-5 zeolite. Because of the relatively large size of confined molecules, the diffusion could be observed within the time window of a backscattering spectrometer only at high temperatures. Branched alkanes were found to diffuse much more slowly than linear alkanes: for example, the diffusion of $CH_3(CH_2)_6CH_3$ at 400 K was significantly faster than that of $CH(CH_3)_3$ at 570 K.

Role of molecular-based simulation

In many experiments, simple structural and dynamic analytical models can provide only

limited insight into the system's properties. For such cases, computer simulations become necessary in order to understand the system's behavior and interpret the experimental results. While a large number of simulation studies of liquids in confinement have been performed, instead of presenting numerous examples we would like to outline some approaches that can be taken when using simulated data.

The data obtained in the course of a simulation (frequently, molecular dynamics) can be used in several ways. The simulated data are often compared directly with experimental data. A typical example is a study by Ricci et al. (2000), who used MD to calculate the radial correlation functions for bulk water and water confined in Vycor glass and compare them with the experimental radial correlation functions. Single-particle diffusional dynamics of water confined in Vycor glass was also calculated in this work. Another very recent example of simulation-experiment synergy was described by Skipper et al. (2006) for behavior of water in clays.

An alternative approach is to analyze simulated data without directly comparing them with an experiment, especially when the experiment would be difficult to perform. For example, Gallo and Rovere (2003) modeled dynamics of water in Vycor glass at low hydration levels. They reported a profound difference between the water molecules near the surface of cylindrical pores and the rest of the confined water molecules. The former exhibited an anomalous diffusion, whereas the latter showed ordinary Brownian motion. Such a distinction may be difficult to assess in an experiment, where constant exchange between molecules near and far from the surface takes place. Another example of an interesting model system which would be difficult to investigate experimentally is a study of water confined to a slab geometry (Zangi 2004).

Some computational studies are used to set up a new framework for interpretation of the whole class of experimental data. For example, molecular dynamics studies by Chen et al. (1999) and Liu et al. (2002) were used to establish the relaxing cage model for water that we have discussed in the previous section. Another example is a discussion of the limits of applicability of the decoupling approximation for rotational and translational diffusion components in water by Faraone et al. (2003a). Similarly, the recent work by Wang et al. (2006) provides MD descriptions of water behavior in a variety of layered minerals including brucite, gibbsite, muscovite, and talc which should be experimentally verified with neutron scattering and other complementary methods such as NMR.

Last but not least, simulation can be used to link results obtained using different experimental techniques and discuss their validity. Malikova et al. (2005, 2006) recently compared computer simulations with QENS and spin-echo neutron measurements of diffusion of water in clays to demonstrate that underestimation of the relaxation times (that is, overestimation of water dynamics) may occur if the limitations of experiment or simulation preclude assessment of sufficiently long relaxation times.

FLUID INTERACTION WITH SURFACES

Many of the chapters included in this volume describe how neutrons can contribute to our understanding of bulk-condensed matter in cases of geological importance and interest. Despite the fact that neutron methods are traditionally viewed as a bulk technique (since they scatter from the nucleus and because of the lower fluxes available at even the most intense neutron sources) they can also be successfully applied to study surfaces and interfaces (e.g., gas-solid, fluid-solid, fluid-fluid and buried interfaces). In an earlier volume of the Reviews in Mineralogy and Geochemistry series Fenter (2002) and Bedzyk and Cheng (2002) discuss how X-ray reflectivity and X-ray standing wave techniques can be used to probe mineral surfaces and interfaces. Here we illustrate how neutron scattering techniques could and have

been used to investigate problems of similar types by presenting several prototypical examples of how diffraction and inelastic scattering techniques have been applied to the study of gas-solid and liquid-solid interfaces and within porous media. The main advantage that neutron techniques offer in this arena is the possibility to study BOTH the structure and the dynamics of the system of interest at the microscopic level. We will discuss how neutron diffraction and inelastic scattering can be used to study the interaction of gases and fluids with lamellar compounds (i.e., graphite and clays), metal oxides and within porous media (such as Vycor glass and nanometer scale tubular arrays). Our objective here is to illustrate the power of the technique and to stimulate the use of neutrons to study of problems relevant to the interest of geochemists.

Structure based on neutron diffraction from layered and two-dimensional systems

While single crystal surfaces and interfaces are readily studied using X-ray and electron diffraction techniques, neutrons can only be applied to such interfacial studies if high surface to volume materials can be used or where large beam footprints are employed such as in reflectometry studies. As noted above, these studies typically involve materials like clays, mica, graphite, and silica. One of the earliest studies relevant to the discussion here is that of Warren (1941) who explained how the diffraction from crystalline powders of random layer materials (like graphite and carbon blacks) exhibits diffraction patterns with characteristic lineshapes that are shaped like a sawtooth. Warren considered a model system composed of a random layer of lattice structures arranged parallel and equidistant from one another, but a random translation parallel to a layer and rotation about the normal. Warren explained his results by noting that the calculated lineshape was a direct result of the powder averaging of a perfect two-dimensional (2D) reciprocal lattice of rods that correspond to the real space "sheets" of carbon that form the basal plane of graphite. Figure 12 (left panel) shows schematically how the asymmetric sawtooth line shape arises while Figure 12 (right panel) is a plot of the diffraction pattern from a randomly oriented material that is a collection of 2D planes. This diffraction profile is often referred to as the "Warren" lineshape. His argument holds true for other lamellar materials as well, so it is relevant to our discussion here.

Since we are considering a 2D system, we note that this is a monomolecular system and all of the centers of mass of the molecules are in the same plane (even if individual nuclei in the molecule are not). $S(Q)$, introduced earlier in this chapter, therefore only depends on the component of Q projected onto the scattering plane, Q_{parallel}. Just as Warren did we now

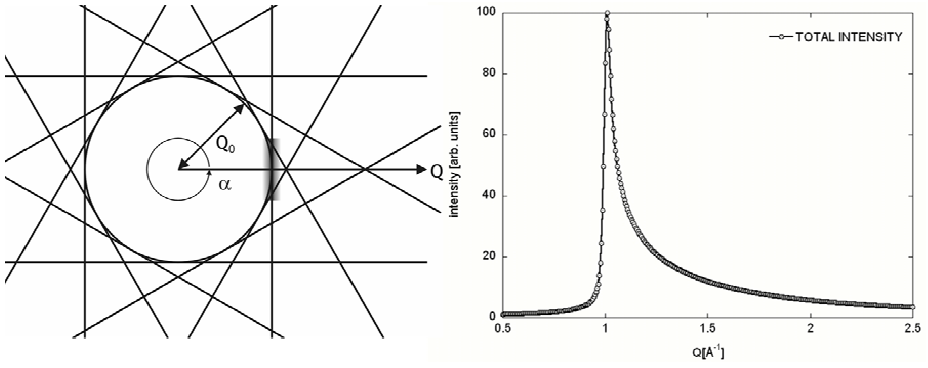

Figure 12. Schematic representation of how the projection of Bragg rods (left panel) leads to the asymmetric shape shown in the Warren lineshape figure illustrated in the right hand panel. The origin of this asymmetry is discussed in the text. This diffraction pattern uses a Lorentzian profile for the structure factor of the Bragg rod.

consider the case of lamellar systems like graphite and mica and assume that the scattering system has random orientations of the crystallites about an axis normal to the basal (or 2D) plane. Because the magnitude of the parallel component of the structure factor S(Q) is the relevant quantity we note that:

$$S(Q_{\text{parallel}}) = \frac{1}{2\pi}\int_0^{2\pi} S(Q_{\text{parallel}},\xi)d\xi \tag{27}$$

where ξ is the angle made by Q_{parallel} with respect to an arbitrary reference direction in the scattering plane. An average must be made over the distribution of the surface normal to the individual crystallites that make up the powdered sample. Figure 13 illustrates the scattering geometry for a single crystallite. This figure shows a crystallite (labeled as the primed coordinate system) where the surface normal (z' axis) is oriented at an angle θ with respect to the unprimed laboratory frame. The primed frame is chosen so that both the primed and unprimed y axes lie in the same plane and the z' axis lies in the yz plane of the lab frame. For this illustration we chose the **Q** vector to be along the y axis. Hence Q_{parallel} can be given by:

$$Q_{parallel} = \left|Q\hat{\mathbf{y}} - (\mathbf{Q}\cdot\hat{\mathbf{z}}')\hat{\mathbf{z}}\right| = Q(1-\sin^2\theta\sin^2\phi)^{1/2} \tag{28}$$

where $\hat{\mathbf{y}}$, $\hat{\mathbf{z}}$ and $\hat{\mathbf{z}}'$ are unit vectors pointing along the respective primed and unprimed axes. We use some straightforward vector geometry to express the unit vector $\hat{\mathbf{z}}'$ in terms of the laboratory (unprimed) frame. If the probability distribution of the crystallite plane normals per unit solid angle is $P(\theta)$ then the fraction of plane normals within the solid angle $\sin\theta d\theta d\phi$ is given by their product $[P(\theta)\sin\theta d\theta d\phi]$. By combining our results from above and assuming that $F(Q)$ (see Eqn. 9a,b) depends only on the magnitude of Q, we find that the cross section can be written as:

$$\frac{d\sigma}{d\Omega} = B^2\left|F(Q)\right|^2\int_0^{2\pi} d\phi\int_0^{\pi} d\theta\sin\theta P(\theta)S[Q(1-\sin^2\theta\sin^2\phi)^{1/2}] \tag{29}$$

While this is the essence of what is required to calculate the cross section it is noteworthy to indicate that Warren deduced that in the vicinity of the two dimensional reciprocal lattice vector τ_{hk} for a finite sized 2D crystallite of coherence length L the structure factor can be approximated by:

$$S(Q) = \rho_0(L/a)^2 e^{-[|Q_{parallel}-\tau_{hk}|^2 L^2/4\pi]} \tag{30}$$

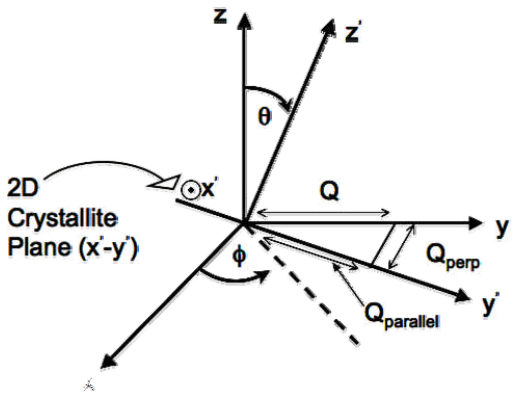

Figure 13. Scattering geometry for a 2D crystallite with the surface normal (z') tilted with respect to the fixed laboratory z axis. Note that the x' axis comes out of the plane of the paper.

Numerous authors have more recently expanded the expression for the cross section given in Equation (29) in various ways. Most of this work is for determining the structure of adsorbed films on solid substrates in particular graphite. The details of these expansions can be found in Stephens et al (1984), Dutta et al. (1980) and Dimon et al. (1985). The work of Dimon et al. (1985) is particularly noteworthy in that it finds that a Lorentzian distribution gives a more satisfactory fit to the lineshape. Our recent experimental evidence suggests that the Lorentzian lineshape can be successfully used to describe the scattering profile of adsorbed molecular films on substrates like graphite foam and MgO where a truly random distribution of the crystallites seems to be realized. Figure 14 illustrates the overall quality of the Lorentzian lineshape description for an a monolayer butane film adsorbed on MgO(100) surfaces. We have focused our attention on describing the lineshape for 2D solid systems, however in cases where the range of spatial correlations is restricted to near neighbor and next near-neighbor coordination rings and where translational mobility also is present (i.e., 2D liquid/fluids), we assume that the reader understands that these lineshapes would broaden in response to the decay of the spatial correlations. Later in this discussion we will indicate how INS and QENS can be used in conjunction with diffraction to gain further microscopic information about the details of the dynamics in interfacial solids and fluids.

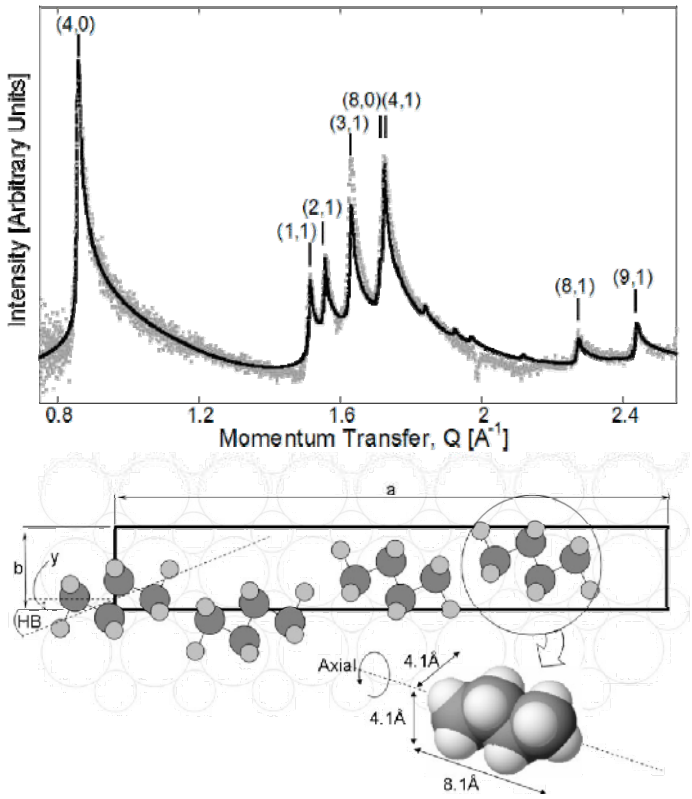

Figure 14. Neutron diffraction study of the structure of a single layer of butane adsorbed to an MgO (100) surface. The sawtooth shaped peaks in the diffraction pattern (upper panel) indicate that the molecular film is two-dimensional. The lower panel illustrates how the four molecules in the unit cell (a = 29.5 Å; b = 4.21 Å) are arranged. The molecules are found to "register" with the MgO lattice with a $2\sqrt{2} \times 7\sqrt{2}$ cell configuration. (Arnold et al. 2006a).

It is of some interest to consider the situation where one of the idealized 2D systems that we have addressed can be followed in a layer by layer growth mode from a strictly 2D plane to one that is more 3D like. Such is the situation in the formation of multilayer molecular films adsorbed to uniform substrates or where epitaxial metal or soft matter growth is realized in chemical vapor deposition, molecular beam epitaxy or polymeric deposition systems. The "lineshape" discussion above has to be modified to account for the development of the third dimension of order in the system. Conceptually this is rather straightforward. Instead of considering, as Warren (1941) did, an ideal 2D reciprocal lattice composed of an ordered array of uniform rods; the reciprocal lattice for an idealized multilayer (e.g., 2-5 individual layer) system is characterized by an array of modulated rods, where the functional form of the modulation of those rods represents the details of the spatial distribution of the scatters in the direction perpendicular to the original 2D plane. Stephens et al. (1984) considered the multilayer diffraction situation in X-ray scattering studies while Larese and his collaborators considered how neutron scattering could be used to follow the growth and melting of atomic and molecular systems on graphite. Figure 15 illustrates how neutron diffraction patterns evolve with film thickness for the growth of ideal two and three layer close-packed films on the graphite basal plane.

Dynamics derived from inelastic neutron scattering

The general concept of using inelastic neutron scattering to obtain information concerning the dynamical properties of condensed matter systems has been covered in numerous places in this volume and for the case of QENS applied to the study of translational diffusion in confined liquids. In the following sections we discuss how rotational and vibrational motions might also be incorporated into these interfacial investigations. For a more detailed discussion of scattering functions characterizing translational diffusion refer to the earlier section on QENS studies of confinement.

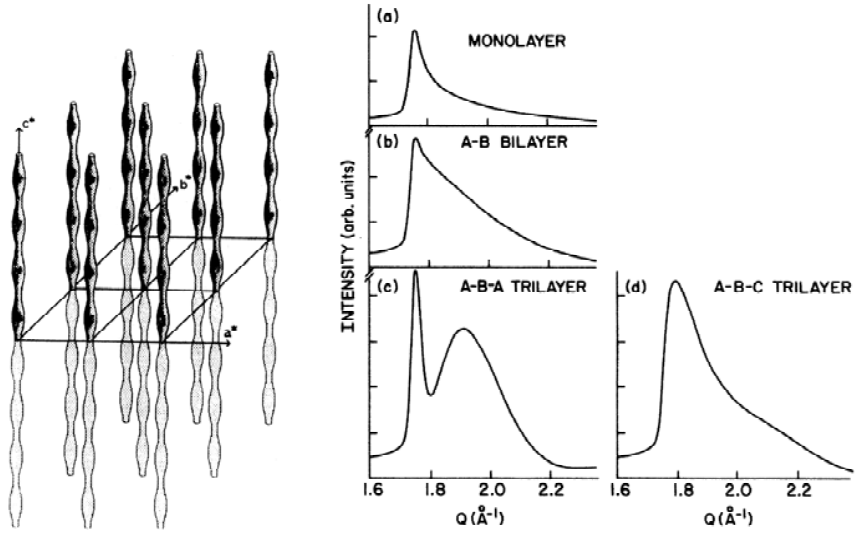

Figure 15. Schematic view (left panel) of a modulated lattice of rods characteristic of a spatially finite bilayer structure. Model line-shape calculations (right panel) for a powder-averaged diffraction profile resulting from an *A-B* stacking sequence for (a) monolayer, (b) bilayer, (c) trilayer thick film, (d) illustrates the diffraction profile for an *A-B-C* trilayer. A triangular, commensurate, close-packed structure was used in each case. The in-plane lattice spacing was the same in all cases. The interplane distance was held fixed between all layers. [Used with permission from Larese et al. (1988a) Phys Rev B, Vol. 37, Figs. 1,2, p. 4736. © by the American Physical Society. URL: *http://link.aps.org/abstract/PRB/v37/p4735*]

Neutron scattering can be applied effectively in the study of the vibrational and rotational motion of hydrogen bearing molecules or molecular species. The large incoherent cross section for hydrogen means that incoherent neutron scattering can also be used for vibrational spectroscopy. The major advantage that neutrons offer as a tool for vibrational spectroscopy over the more common optical techniques of infrared and Raman scattering is that there are no symmetry-dependent selection rules that cause certain modes to be unobservable. A very recent monograph by Mitchell et al. (2005) is an excellent and practical resource for gaining a foundation and understanding of neutron vibrational spectroscopy as it has been applied in chemistry, biology, materials science and catalysis. While it is clear that we need to once again consider the neutron scattering cross section, we will simplify this discussion here and point out that information about the normal modes of vibration of a molecule or of molecules attached to a surface or chemically bound to an interface can be realized using the incoherent scattering (we will not discuss the measurements of phonons in crystals or collective vibrations here but naturally these can be measured). The intensity of the i^{th} molecular vibrational transition is proportional to:

$$I_i \propto Q^2 U_i^2 e^{-Q^2 U_{total}^2} \sigma \tag{31}$$

where U_i is the vibrational amplitude of the atoms within the particular mode. The exponential term in Equation (31) is the Debye-Waller factor and U_{total} is the mean square displacement of the molecule. The magnitude of this is partially determined by the thermal motion of the molecule. A very good example of how this type of spectroscopy can be used in the mineralogical context is shown in Figure 16 (Dove 2002).

Another important dynamical process which neutrons can probe is the characterization of rotational motion. If a molecule rotates randomly about its center of mass (COM), the positions of the hydrogen atoms $\mathbf{r_n}(t)$ move over a sphere of constant radius $|\mathbf{r_n}|$. This type of motion is referred to as rotational diffusion. For illustrative purposes, consider the simple case of the diffusion of a single-atom-bearing molecule that is rotationally diffusing. Such a model would be a reasonably good choice for a system like crystalline methane at temperatures just below the

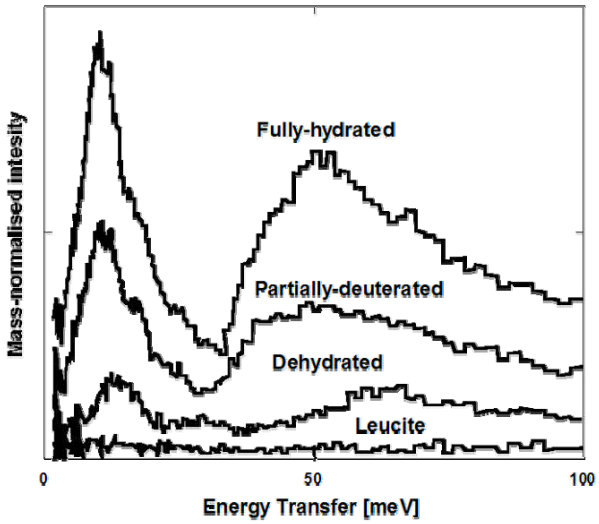

Figure 16. Incoherent inelastic neutron scattering from samples of analcime with various degrees of hydration and compared with scattering from leucite. [Used by permission of Schweizerbart Science Publishers (*http://www.schweizerbart.de*), from Dove (2002), Euro J Min, Vol. 14, Fig. 12, p.218]

melting point. Here the molecular COM is fixed on a lattice but the molecules are freely reorienting. One finds that a rate law similar to the one applicable to translational diffusion exists:

$$\frac{\partial G}{\partial t} = D_R \nabla_\Omega^2 G \tag{32}$$

where G is the time dependant angular probability function and D_R is the rotational diffusion constant, the inverse of which gives the time constant for rotational motion. It is convenient to express the operator ∇^2 in spherical coordinates. While the expression seems rather straightforward, the complexity of the actual solution is significant. As with the expression for translation diffusion the result can found in the monograph by Bee (1988). The solution is:

$$G\left[\Omega(t)\Omega(0)\right] = 4\pi \sum_{t=0}^{\infty} e^{-(D_R l(l+1)t)} \sum_{m=-l}^{+l} Y_m^l\left[\Omega(t)\right] Y_m^{l*}\left[\Omega(0)\right] \tag{33}$$

where the $Y^l{}_m(\Omega)$ are the spherical harmonics and $G[\Omega(t),\Omega(0)]$ is the probability of finding the bond orientation at $\Omega(t)$ at time t; when it is at $\Omega(0)$ at time $t = 0$. The intermediate scattering function takes the form:

$$F_{\mathrm{inc}}(Q,t) \propto j_0^2(Qr) + \frac{1}{\pi}\sum_{l=1}^{\infty}(2l + j_l^2(Qr) e^{-\left[D_R l(l+1)\right]} \tag{34}$$

where j_l's are the regular Bessel functions. The incoherent scattering function is derived immediately from the Fourier transform as:

$$S(Q,\omega) \propto j_0^2(Qr)\delta(\omega) + \frac{1}{\pi}\sum_{l=1}^{\infty}(2l+1) j_l^2(Qr) \frac{D_R l(l+1)}{\left[D_R l(l+1)\right]^2 + \omega^2} \tag{35}$$

where $\delta(\omega)$ is the Dirac delta function. Notice that the expression has two parts, the (l = 0) component which is the elastic line centered at $\omega = 0$ and the second one which is a summation of Lorentzian peaks with widths independent of Q. The lowest order term in the latter component ($L = 1$) has a width of $2D_\mathrm{R}$, whereas higher order terms have greater widths. The amplitudes of the quasielastic components are Q dependent via the Bessel functions. The temperature dependence of the QENS component often follows an Arrhenius relation:

$$\tau^{-1} = D = D_0 e^{(-E_R/RT)} \tag{36}$$

where E_R is the activation energy related to the rotational motion (see Fig. 17).

While we have shown that the quasi-elastic component of the incoherent scattering is useful for determining the time constant for rotational diffusion, the elastic incoherent component can also be used to obtain useful information concerning the position of the hydrogen atoms. The elastic component can be used to define the Elastic Incoherent Structure Factor (EISF) or $\mathrm{I_{EISF}}(Q)$ which is:

$$I_{\mathrm{EISF}}(Q) = \frac{S_{el}(Q)}{S_{el}(Q) + S_{qe}(Q)} \tag{37}$$

For isotropic rotational motion of molecules with radius r, the EISF has the simple form:

$$I_{\mathrm{EISF}}(Q) = \frac{\sin(Qr)}{Qr} \tag{38}$$

The EISF has been used to better understand the nature of the rotational dynamics in a wide range of interfacial systems. In Figure 18 we show one such study of EISF reported by Simon et al. (1990) on nitric acid intercalated in graphite.

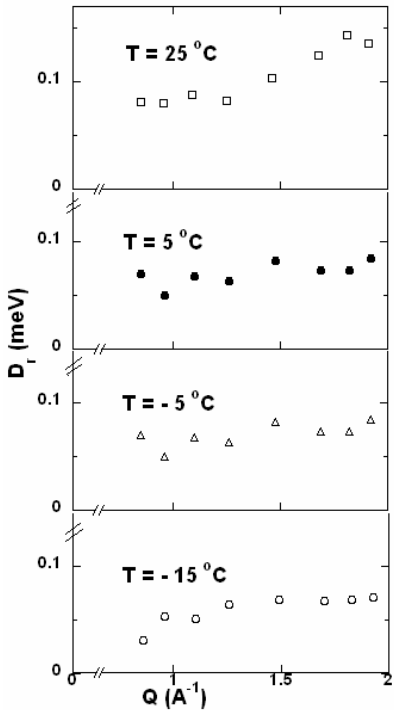

Figure 17. The rotational linewidth as a function of Q for four temperatures for the rotational diffusion of water in Vycor glass. [Reprinted with permission from Bellissent-Funel et al. (1995), Phys Rev E Vol. 51, Fig. 7, p.4565. © 1995 American Physical Society. URL: *http://link.aps.org/abstract/PRE/v51/p4558*]

It is commonly found that at lower temperatures or when the barrier to rotation is high (i.e., the rotational motions are significantly hindered) neutrons have been used to study the discrete transitions between rotational levels, librational motion and quantum (rotational) tunneling. A recent review article by Johnson and Kearley (2000) and the monograph by Press (1981) should be consulted for an introduction to this topic. The extreme sensitivity of the tunnel spectrum to the potential energy surface (PES) demonstrates that high resolution neutron spectroscopy provides a unique probe of intermolecular interactions that is unrivalled in its sensitivity to the potential energy landscape. Molecular groups that exhibit rotational tunneling provide a direct measure of the symmetry and magnitude of intermolecular and weak intramolecular interactions (comparable to the thermal energy kT at room temperature). Tunneling (translational) is purely a quantum phenomenon familiar to all beginning students of quantum mechanics in the study of the particle in a box. The rotational analogue is easily understood by considering molecules in a lattice where local barriers to rotation are too great for classical reorientation of the molecule to take place. The simplest example for us to consider here is where the rotation is one-dimensional—e.g., a methyl group rotor. Here it is sufficient to consider a single coordinate ϕ, used to describe the angular coordinate of the symmetrically distributed triangle of hydrogen

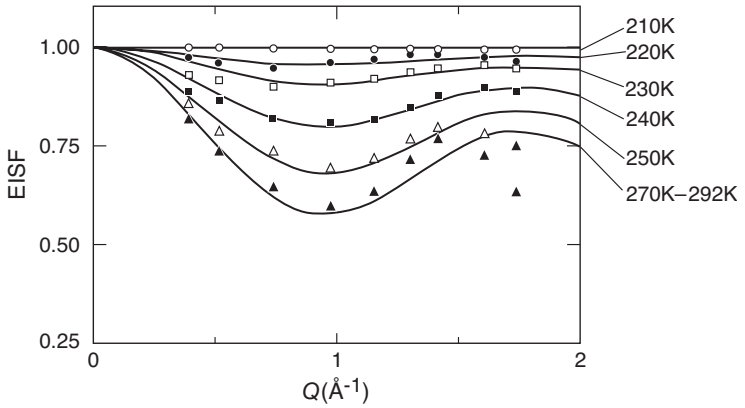

Figure 18. EISF for in-plane rotation of the nitric acid molecule intercalated in graphite. [Reprinted with permission from Simon et al. (1990), Phys Rev B, Vol. 41, Fig. 4, p.2393. © 1990 American Physical Society. URL: *http://link.aps.org/abstract/PRB/v41/p2390*]

atoms, around the central carbon atom (i.e., the C_{3v} axis of the CH_3 group). The Hamiltonian for this single particle motion is given by Mitchell et al. (2005):

$$\frac{h^2}{4\pi I}\frac{\partial^2}{\partial\phi^2}+\sum_{n\geq 1}\frac{V_{3n}}{2}\{1+\cos[3n(\phi+\alpha_{3n})]\}=\frac{h^2}{4\pi I}\frac{\partial^2}{\partial\phi^2}+\sum_{n} b_n e^{i3n\phi} \tag{39}$$

where $I = 3mr^2$ is the moment of inertia for three hydrogen atoms of mass, m and displaced from the axis of rotation by the radius, r. The potential energy is expressed as a Fourier series, typically limited to $n \leq 2$, in which case experimental data are required to determine three parameters, V_3, V_6, and the relative phase, $\alpha = \alpha_6 - \alpha_3$. A basis set of free rotor wave functions can be used with the Hamiltonian and diagonalized to obtain a set of tunneling and vibrational (librational) energy levels and wave functions. In Figure 19 (from Johnson and Kearley 2000) the rotational potential is shown in the upper panel along with a schematic energy levels for a methyl rotor. Notice that each librational level is split into a singlet and a doublet, with symmetry species A and E, respectively. It is interesting to observe that there is an exponential decay of the tunnel splitting while there is a nearly linear increase in libration frequency as a function of barrier height are illustrated in the lower panel of Figure 19. The strength of the rotational potential at which the free rotor description (on the *left* of the lower panel) becomes tunneling is arbitrarily taken to be at about 2 meV (20 K). While tunneling data can be used to precisely define the PES, it is not true that this is a simple process once the rotor goes beyond a 1D type.

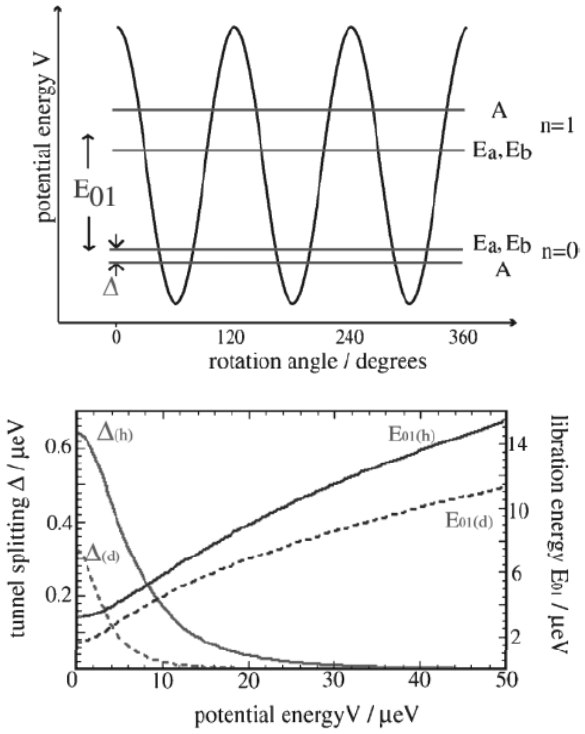

Figure 19. (upper panel) A simple rotational potential and corresponding tunnel split energy levels for the two lowest energy librational levels $n = 0,1$. (lower panel) The tunnel splitting Δ and librational frequencies are shown as a function of the rotational hindering potential V for CH_3 and CD_3 with the solid and broken lines, respectively. [Used by permission of Annual Reviews, from Johnson and Kearley (2000), Ann Rev Phys Chem, 51, Fig. 1, p. 297-321]

Neutron diffraction and inelastic scattering in the study of the adsorbed films

Numerous neutron diffraction studies of adsorbed molecular films on or intercalated between the graphite basal planes, and on the lamellar halides, clays and MgO have been performed over the last three decades. The bulk of these studies were aimed at answering questions concerning the nature of 2D solids, solid-solid and solid-liquid phase transitions (especially KTHNY melting), layer-by-layer growth, preferential adsorption, and orientational ordering. Here we highlight only a few examples relevant to geochemistry and mineralogy, but encourage the interested reader to consult the conference proceedings (Sinha, 1980; Taub et al. 1991) and monograph (Bruch et al. 1997) for more information.

Graphite and carbonaceous materials

A surge of neutron (and subsequently X-ray) diffraction studies on the structure of adsorbed films on graphite followed the pioneering work of Passell and his coworkers (Kjems et al. 1976) in the 1970's. Using a simple difference technique, Passell was first to show that a non-surface specific probe like neutrons was excellent for the study of the structure and dynamics of adsorbed films. Sheets formed from compressed powders of crystalline graphite distributed under the trade names Grafoil (Union Carbide) and Papyex (Le Carbone Lorraine) were found to be ideal candidates for these "surface" studies. The largest concentration of neutron scattering studies of the structure and dynamics of these adsorbed phases has focused on adsorbed hydrocarbons. Much of the early work determined both the structure of these 2D solid phases and the nature of the melting transition for 2D films (Dash 1999; Hansen and Taub 1999). This is a special type of confined system since the behavior is nominally 2D. A concerted effort was made in the late 70's to the mid 80's to gather evidence to support the predictions by Kosterlitz and Thouless (1973), Halperin and Nelson (1979) and Young (1979)—the (KTHNY) theory—that melting in 2D proceeds via a two step, continuous process that involves a bond ordered state known as the "hexatic phase" that intervenes between the solid and usual isotropic liquid phase. Strandberg (1988) has written an excellent review of 2D melting and the reader is directed there for additional information. Perhaps the most extensively studied system from the stand point of continuous melting in 2D and of layering transitions involves the ethylene-on-graphite system (Kim et al. 1986; Larese et al. 1988b). Also relevant to interfacial or liquids in restricted geometries are the studies of surface melting and reentrant layering (Herwig et al. 2000). These studies are particularly important because they establish that interfacial solids can be stabilized at the adsorbate-film interface when additional liquid layers are adsorbed above them. Neutron scattering studies of layer-by-layer melting of rare gas solids by Larese (1993) and Phillips et al. (1993), and of alkane films (Arnold et al. 2002a,b), carboxylic acids (Bickerstaffe et al. 2004) and alkane-alcohol mixtures by Messe et al. (2005) have firmly established that this fascinating behavior appears in a wide range of fluid-solid interfacial systems.

MgO

Metal oxides are important compounds not only industrially but also as components of earth materials. This coupled with the fact that the next major component of the geosphere is water suggests that neutron studies of structure and dynamics of adsorbed films and interfacial water on metal oxides could act as a prototype for the study of more complex mineralogical systems. After adsorption on graphite perhaps the next most intensely studied system where 2D and interfacial phenomena discussed above has been investigated is magnesium oxide. While work by Coulomb et al. (1984) stimulated a number of papers in the 1980's, production of MgO powders in sufficient quantities to supply a large number of research groups was not available. Thanks to the recent interest in nanoscience and new synthetic methods for the production of large quantities of nanometer scale nanocubes of MgO a resurgence of the structure and dynamics of small molecular systems including methane and other n-alkanes

(Arnold et al. 2005, 2006b), hydrogen (Larese et al. 2006) and water have recently started to appear in the literature. One such study is a combined experimental and theoretical investigation of the rotational tunneling of methane on MgO (100) surfaces. Figure 20 shows the rotational tunneling spectrum for a monolayer film of methane measured using high resolution inelastic neutron scattering.

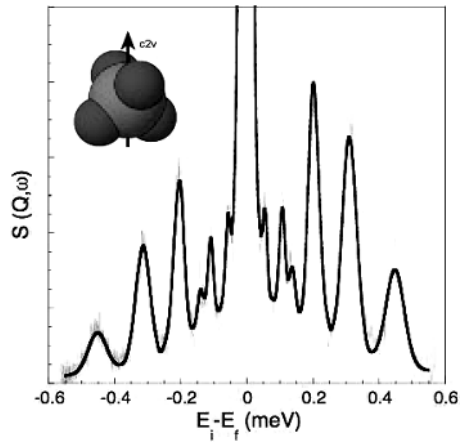

Figure 20. Inelastic neutron "rotational tunneling" spectrum collected at 1.5 K from a single layer of methane adsorbed to a MgO(100) surface. Analysis of this spectrum leads to the surprising result that methane sits in the "dipod" configuration, i.e., with its C_{2v} axis normal to the surface plane, as shown in the inset. [Reprinted with permission from Larese et al. (2001) Phys Rev Lett, Vol. 87, Fig. 1, p. 206102-2. © 2001 by the American Physical Society. URL: *http://link.aps.org/abstract/PRL/v87/e206102*]

SUMMARY AND FUTURE DIRECTIONS

There can be no disputing the fact that neutron diffraction and scattering have made a clear contribution to our current understanding of the structural and dynamical characteristics of liquid water and water containing dissolved ions at ambient conditions and to a somewhat lesser degree other state conditions involving a change in temperature and pressure. Indeed, a molecular-level understanding of how fluids (e.g., water, CO_2, CH_4, higher hydrocarbons, etc.) interact with and participate in reactions with other solid earth materials are central to the development of predictive models that aim to quantify a wide array of geochemical processes. The importance of the hydrogen-bond interaction, in water and other important hydrogenous fluids, has been highlighted as well as the sensitivity of the network to perturbations by a change in physical conditions or proximity to solute molecules and interfaces. Despite the large body of work that documents the nature of hydrogen bonding and associated interactions with its local surroundings, it is premature to assume that we have a complete understanding of the mechanisms that give rise to the particular properties exhibited by water and other simple molecular fluids. This is particularly true as one goes both above and below ambient conditions. For example, there is continuing discussion on the relation between the behavior of supercooled water, the structure of the amorphous ices, the behavior of molecular fluids at interfaces and the incorporation of simple molecules in hydrate clathrates. This is of particular interest since we have seen that nanoporous confinement of water at ambient conditions leads to structural and dynamical features that emulate the super-cooled state. In the context of natural systems, interrogation of fluids and fluid-solid interactions at elevated temperatures and pressures is an area requiring much more work, particularly for complex solutions containing geochemically relevant cations, anions, and other important dissolved species such CO_2 or CH_4. We have tried to describe a series of prototypical interfacial and surface problems using neutron scattering to stimulate the thinking of earth scientists interested applying some of these approaches to confined systems of mineralogical importance.

Our ability to predict the molecular-level properties of fluids and fluid-solid interactions relies heavily on the synergism between experiments such as neutron diffraction or inelastic neutron scattering and molecular-based simulations. Tremendous progress has been made in closing the gap between experimental observations and predicted behavior based on simulations due to improvements in the experimental methodologies and instrumentation on the one hand, and the development of new potential models of water and other simple and complex fluids on the other. For example there has been an emergence of studies taking advantage of advanced computing power that can accommodate the demands of *ab initio* molecular dynamics. On the neutron instrumentation side while much of the quasielastic work described above has been performed using instrumentation located at reactor based sources, the advent of 2nd generation spallation neutron sources like ISIS, new generation sources like the SNS at the Oak Ridge National Laboratory and the low repetition rate 2nd target station at ISIS offer significant opportunities for the study of interfacial and entrained liquids. At the very least, an improvement of the counting statistics by one to two orders of magnitude on many instruments such as vibrational and time-of-flight spectrometers at SNS will allow parametric studies of many systems which otherwise would be prohibitively time consuming. The extended-Q SANS diffractometer at SNS will offer very high intensity and unparalleled Q-range to extend the accessible length scale in the real space, from 0. 05 nm to150 nm. The backscattering spectrometer will provide very high intensity and excellent energy resolution through unprecedented range of energy transfers, thereby allowing simultaneous studies of translational and rotational diffusion components in various systems. The vibrational spectrometer with two orders of magnitude improvement in performance and the capability to perform simultaneous structural measurements should present exciting opportunities to and engender an entire new population of users in the neutron community.

ACKNOWLEDGMENTS

Research by DRC was sponsored by the Division of Chemical Sciences, Geosciences, and Biosciences, Office of Basic Energy Sciences (OBES), U.S. Department of Energy, under contract DE-AC05-00OR22725, Oak Ridge National Laboratory, managed by UT-Battelle, LLC. KWH and EM acknowledge support to SNS from the U.S. Department of Energy, under contract DE-AC05-00OR22725, Oak Ridge National Laboratory, managed by UT-Battelle, LLC. JZL gratefully acknowledges support from OBES, Division of Materials Sciences and Engineering under contract DE-AC05-00OR22725, and NSF under DMR-0412231. The authors would like to thank Drs. H.-R. Wenk, C. J. Benmore, A. A. Chialvo and J. M. Simonson for their constructive comments, R. Violet for help in assembling references for the chapter, and D. Cottrel for redrawing a number of the figures.

REFERENCES

Agamalian M, Drake JM, Sinha SK, Axe JD (1997) Neutron diffraction study of the pore surface layer of Vycor glass. Phys Rev E 55:3021-3027

Alba-Simionesco C, Dosseh G, Dumont E, Frick B, Geil B, Morineau D, Teboul V, Xia Y (2003) Confinement of molecular liquids: Consequences on thermodynamic, static and dynamical properties of benzene and toluene. Eur Phys J E 12:19-28

Ansell S, Neilson GW (2000) Anion-anion pairing in concentrated aqueous lithium chloride solution. J Chem Phys 112:3942-3944

Ansell S, Tromp RH, Neilson GW (1995) The solute and aquaion structure in a concentrated aqueous solution of copper(II) chloride. J Phys Condens Matter 7:1513-1524

Arnold T, Chanaa S, Cook R, Clarke SM, Larese, JZ (2006a) The structure of N-butane monolayer adsorbed on an MgO(110). Phys Rev B (in press)

Arnold T, Cook RE, Chanaa S, Clarke SM, Farinelli, PY, Larese JZ (2006b) Neutron scattering and thermodynamic investigations of thin films of n-alkanes adsorbed on MgO(100) surfaces. Phys Rev B (in press) doi: 10.1016/j.physb.2006.05.189

Arnold T, Cook RE, Larese JZ (2005) Thermodynamic investigation of thin films of ethane adsorbed on magnesium oxide. J Phys Chem B 109:8799-8805

Arnold T, Dong CC, Thomas RK, Castro MA, Perdigon A, Clarke SM, Inaba A (2002a) The crystalline structures of odd alkanes pentane, heptane, nonane, undecane, tridecane and pentadecane adsorbed on graphite at submonolayer coverages and from liquid. Phys Chem Chem Phys 4:3430-3435

Arnold T, Thomas RK, Castro MA, Clarke SM, Messe L, Inaba A (2002b) The crystalline structures of even alkanes hexane, octane, decane, dodecane and tetradecane monolayers adsorbed on graphite at submonolayer coverages and from liquid. Phys Chem Chem Phys 4:345-351

Badyal YS, Simonson JM (2003) The effects of temperature on the hydration structure around Ni^{2+} in concentrated aqueous solutions. J Chem Phys 119:4413-4418

Baker JM, Dore JC, Behrens P (1997) Nucleation of ice in confined geometry. J Phys Chem B 101:6226-6229

Bär NK, Ernst H, Jobic H, Kärger J (1999) Combined quasi-elastic neutron scattering and NMR study of hydrogen diffusion in zeolites. Magn Reson Chem 37:S79-S83

Bedzyk ML, Cheng L (2002) X-ray standing wave studies of minerals and mineral surfaces: principles and applications. Rev Mineral Geochem 49:221-266

Bée M (1988) Quasielastic Neutron Scattering. Adam-Hilger

Bellissent-Funel MC (1998) Is there a liquid-liquid phase transition in supercooled water? Europhys Lett 42: 161-166

Bellissent-Funel MC (2001) Structure of supercritical water. J Molec Liq 90:313-322

Bellissent-Funel MC, Bosio L (1995) A neutron scattering study of liquid D_2O under pressure and at various temperatures. J Chem Phys 102:3727-3735

Bellissent-Funel MC, Bradley KF, Chen SH, Lal J, Teixeira J (1993) Slow dynamics of water molecules in confined space. Physica A 201:277-285

Bellissent-Funel MC, Chen SH, Zanotti J-M (1995) Single-particle dynamics of water molecules in confined space. Phys Rev E 51:4558-4569

Bellissent-Funel MC, Lal J, Bosio L (1992) Structural study of water confined in porous glass by neutron scattering. J Chem Phys 98:4246-4252

Bellissent-Funel MC, Teixeira J (1991) Dynamics of water studies by coherent and incoherent inelastic neutron scattering. J Molec Struc 250:213-230

Bellissent-Funel MC, Teixeira J, Bosio L, Dore JC (1989). A structural study of deeply supercooled water. J Phys Condens Matter 1(39):7123-7129

Benes NE, Jobic H, Verweij H (2001) Quasi-elastic neutron scattering study of the mobility of methane in microporous silica. Microporous Mesoporous Mater 43:147-152

Beta IA, Bohlig H, Hunger B (2004) Structure of adsorption complexes of water in zeolites of different types studied by infrared spectroscopy and inelastic neutron scattering. Phys Chem Chem Phys 6:1975-1981

Beta IA, Herve J, Geidel E, Bohlig H, Hunger B (2001) Inelastic neutron scattering and infrared spectroscopic study of furan adsorption on alkali-metal cation-exchanged faujasites. Spectrochem Acta A 57:1393-1403

Beta IA, Li JC, Bellissent-Funel MC (2003) A Quasi-elastic neutron scattering study of the dynamics of supercritical water. Chem Phys 292:229-234

Bickerstaffe A, Messe L, Clarke SM, Perdigon A, Cheah N, Inaba A (2004) Mixing behaviour of carboxylic acids adsorbed on graphite. Phys Chem Chem Phys 6:3545-3550

Bondarenko GV, Gorbaty YE (1973) Infrared spectra of v3 water-d1 at high pressures and temperatures. Dolk Phys Chem 210:369-371

Bosio L, Teixeira J, Bellissent-Funel MC (1989) Enhanced density fluctuations in water analyzed by neutron scattering. Phys Rev A 39:6612-6613

Botti A, Bruni F, Imberti S, Ricci MA, Soper AK (2004) Ions in water: The microscopic structure of a concentrated HCl solution. J Chem Phys 121:7840-7848

Botti A, Bruni F, Isopo A, Ricci MA, Soper AK (2002) Experimental determination of the site - site radial distribution functions of supercooled ultrapure bulk water. J Chem Phys 117:6196-6199

Botti A, Bruni F, Ricci MA, Soper AK (1998) Neutron diffraction study of high density supercritical water. J Chem Phys 109:3180-3184

Broseta D, Barré L, Vizika O, Shahidzadeh N, Guilbaud J-P, Lyonnard S (2001) Capillary condensation in a fractal porous medium. Phys Rev Lett 86:5313-5316

Brown GE, Henrich VE, Casey WH, Clark DL, Eggleston C, Felmy A, Goodman DW, Gratzel M, Maciel G, McCarthy MI, Nealson KH, Sverjensky DA, Toney MF, Zachara JM (1999) Metal-oxide surfaces and their interactions with aqueous solutions and microbial organisms. Chem Rev 99:77-174

Bruch LW, Cole MW, Zaremba E (1997) Physical adsorption: Forces and Phenomena. Intl Series Mono Chem No. 33. Oxford University Press

Bruni F, Ricci MA, Soper AK (1996) Unpredicted density dependence of hydrogen bonding in water found by neutron diffraction. Phys Rev B 54:11876-11879

Bruni F, Ricci MA, Soper AK (1998) Water confined in Vycor glass. I. A neutron diffraction study. J Chem Phys 109:1478-1485

Bruni F, Ricci MA, Soper AK (2001) Structural characterization of NaOH aqueous solution in the glass and liquid states. J Chem Phys 114:8056-8063

Chen SH, Gallo P, Bellissent-Funel MC (1995) Slow dynamics of interfacial water. Can J Phys 73:703-709

Chen SH, Liao C, Sciortino F, Gallo P, and Tartaglia P (1999) Model for single-particle dynamics in supercooled water. Phys Rev E 59:6708-6714

Chen SH, Teixeira J (1986) Structure and dynamics of low-temperature water as studied by scattering techniques. Adv Chem Phys 64:1-45

Chen SH, Teixeira J, Nicklow R (1982) Incoherent quasielastic neutron scattering from water in supercooled regime. Phys Rev E 26:3477-3482

Chialvo AA, Cummings PT (1998) Supercritical water and aqueous solutions: molecular simulation. *In*: Encyclopedia of Computational Chemistry. Scheyer PR (ed) Wiley & Sons, 4:2839-2859

Chialvo AA, Cummings PT, Simonson JM, Mesmer RE, Cochran HD (1998) Interplay between molecular simulation and neutron scattering in developing new insights into the structure of water. Ind Eng Chem Res 37:3021-3025

Chialvo AA, Simonson JM (2006) Ion association in aqueous LiCl solutions at high concentration: Predicted results via molecular simulation. J Chem Phys 124:154509-1–154509-9

Cole DR, Gruszkiewicz MS, Simonson JM, Chialvo AA, Melnichenko YB, et al. (2004) Influence of nanoscale porosity on fluid behavior. *In:* Water-Rock Interaction 1. Want R, Seal R (eds) p 735-739

Colmenero J, Arbe A, Alegria A, Monkenbusch M, Richter D (1999) On the origin of the non-exponential behavior of the α-relaxation in glass-forming polymer: incoherent neutron scattering and dielectric relaxation results. J Phys Condens Matter 11:A363-A370

Corsaro C, Crupi V, Longo F, Majolino D, Venuti V, Wanderlingh U (2005) Mobility of water in Linde type A synthetic zeolites: an inelastic neutron scattering study. J Phys Condens Matter 17:7925-7934

Coulomb J-P, Sullivan TS, Vilches OE (1984) Adsorption of Kr, Xe and Ar on highly uniform MgO smoke. Phys Rev B 30:4753-4760

Crupi V, Dianoux AJ, Majolino D, Migliardo P, Venuti V (2002a) Dynamical response of liquid water in confined geometry by laser and neutron spectroscopies. Phys Chem Chem Phys 4:2768-2773

Crupi V, Majolino D, Migliardo P, Veniti V (2002b) The puzzle of liquid water diffusive behavior: recent IQENS results. Physica A 304:59-64

Crupi V, Majolino D, Migliardo P, Venuti V (2002c) Neutron scattering study and dynamic properties of hydrogen-bonded liquids in mesoscopic confinement. 1. The water case. J Phys Chem B 106:10884-10894

Crupi V, Majolino D, Migliardo P, Venuti V, Dianoux AJ (2002d) Low-frequency dynamical response of confined water in normal and supercooled regions obtained by IINS. Appl Phys A 74:S555-S556

Crupi V, Majolino D, Migliardo P, Venuti V, Mizota T (2004a) Vibrational and diffusional dynamics of water in Mg50-A zeolites by spectroscopic investigation. Mol Phys 102:1943-1957

Crupi V, Majolino D, Migliardo P, Venuti V, Wanderlingh U, Mizota T, Telling M (2004b) Neutron scattering study and dynamic properties of hydrogen-bonded liquids in mesoscopic confinement. 2. The zeolitic water case. J Phys Chem B 108:4314-4323

Crupi V, Majolino D, Venuti V (2004c) Diffusional and vibrational dynamics of water in NaA zeolites by neutron and Fourier transform infrared spectroscopy. J Phys Condens Matter 16:S5297-S5316

Cunsolo A, Orecchini A, Petrillo C, Sacchetti F (2006) Quasieleastic neutron scattering investigation of the pressure dependence of molecular motions in liquid water. J Chem Phys 124:084503-1 – 084503-7

Danielewicz-Ferchmin I, Ferchmin AR (2004) Water at ions, biomolecules and charged surfaces. Phys Chem Liq 42:1-36

Dash JG (1999) History of the search for continuous melting. Rev Mod Phys 71:1737-1743

David F, Vokhmin V, Ionova G (2001) Water characteristics depend on the ionic environment. Thermodynamics and modelization of the aquo ions. J Molec Liq 90:45-62

Davidson AM, Mellot CF, Eckert J, Cheetham AK (2000) An inelastic neutron scattering and NIR-FT Raman spectroscopy study of chloroform and trichloroethylene in faujasites. J Phys Chem B 104:432-438

de Jong PHK, Neilson GW (1996) Structural studies of ionic solutions under critical conditions. J Phys Condens Matter 8:9275-9279

de Jong PHK, Neilson GW (1997) Hydrogen-bond structure in an aqueous solution of sodium chloride at sub- and supercritical conditions. J Chem Phys 107:8577-8585

de Siqueira AV, Lobban C, Skipper NT, Williams GD, Soper AK, Done R, Dreyer JW, Humphreys RJ, Bones JAR (1999) The structure of pore fluids in swelling clays at elevated pressures and temperatures. J Phys Condens Matter 11:9179-9188

Dierker SB, Wiltzius P (1991) Statics and dynamics of a critical binary fluid in a porous medium. Phys Rev Lett 66:1185-1188

Dimon P, Horn PM, Sutton M, Birgneau RJ, Moncton DE (1985) First-order and continuous melting in a two-dimensional system: Monolayer xenon on graphite. Phys Rev B 31:437-447

Dore JC (1984) Neutron diffraction studies of water in the normal and super-cooled liquid phase. J Physique C 7:C7-49–C7-64

Dore JC (1985) Structural studies of water by neutron diffraction. Water Sci Rev 1:3-92

Dore JC (1991) Structural studies of water and other hydrogen-bonded liquids by neutron diffraction. J Molec Struc 250:193-211

Dore JC (2000) Structural studies of water in confined geometry by neutron diffraction. Chem Phys 258:327-347

Dore JC, Garawi M, Bellissent-Funel MC (2004) Neutron diffraction studies of the structure of water at ambient temperatures, revisited [a review of past developments and current problems]. Molec Phys 102: 2015-2035

Dore JC, Sufi MAM, Bellissent-Funel MC (2000) Structural change in D_2O as a function of temperature: The isochoric temperature derivative function for neutron diffraction. Phys Chem Chem Phys 2:1599-1602

Dore JC, Webber B, Hartl M, Behrens P, Hansen T (2002) Neutron diffraction studies of structural phase transformation for water-ice in confined geometry. Physica A 314:501-507

Dove MT (2002) An introduction to the use of neutron scattering methods in mineral sciences. Eur J Min 14: 203-224

Dutta P, Sinha SK, Vora P, Nielson M, Passell L, Bretz M (1980) Neutron diffraction of melting on physisorbed monolayers of methane-d4 on graphite. *In*: Ordering in Two Dimensions. Sinha SK (ed) North Holland Pub, p 169-174

Egelstaff PA (1967) An Introduction to the Liquid State. Academic Press

Egelstaff PA (1992) Illustrations of radiation scattering data. NATO ASI Series C 379:29-44

Egelstaff PA, Polo JA, Root JH, Hahn LJ, Chen SH (1981) Structural rearrangements in low-temperature heavy water. Phys Rev Lett 47:1733-1736

Enderby JE (1983) Neutron scattering from ionic solutions. Ann Rev Phys Chem 34:155-185

Enderby JE (1995) Ion solvation via neutron scattering. Chem Soc Rev 24:159-168

Enderby JE, Cummings S, Herdman GJ, Neilson GQ, Salmon PS, Skipper N (1987) Diffraction and study of aqua ions. J Phys Chem 91:5851-5858

Faraone A, Chen SH, Fratini E, Baglioni P, Liu L, Brown C (2002) Rotational dynamics of hydration water in dicalcium silicate by quasielastic neuron scattering. Phys Rev E 65:040501-1–040501-4

Faraone A, Liu L, Chen SH (2003a) Model for the translation-rotation coupling of molecular motion in water. J Chem Phys 119:6302-6313

Faraone A, Liu L, Mou C-Y, Shih P-C, Brown C, Copley JRD, Dimeo RM, Chen SH (2003b) Dynamics of supercooled water in mesoporous silica matrix MCM-48-S. Eur Phys J E 12:S59-S62

Faraone A, Liu L, Mou C-Y, Shih P-C, Copley JRD, Chen SH (2003c) Translational and rotational dynamics of water in mesoporous silica materials: MCM-41-S and MCM-48-S. J Chem Phys 119:3963-3971

Fawcett WR (2004) Liquids, Solutions, And Interfaces – From Classical Macroscopic Descriptions To Modern Microscopic Details. Oxford

Fenter PA (2002) X-ray reflectivity as a probe of mineral-fluid interfaces: A user guide. Rev Mineral Geochem 49:150-216

Finney JL, Soper AK (1994) Solvent structure and perturbations in solutions of chemical and biological importance. Chem Soc Rev 23:1-10

Floquet N, Coulomb JP, Dufau N, Andre G (2004) Structure and dynamics of confined water in $AlPO_4$-5 zeolite. J Phys Chem B 108:13107-13115

Fratini E, Chen SH, Baglioni P, Bellissent-Funel MC (2001) Age-dependent dynamics of water in hydrated cement paste. Phys Rev E 64:020201-1–020201-4

Fratini E, Chen SH, Baglioni P, Cook JC, Copley JRD (2002) Dynamic scaling of quasielastic neutron scattering spectra from interfacial water. Phys Rev E 65:010201-1–010201-4

Frisken BJ, Cannell DS, Lin MY, Sinha SK (1995) Neutron-scattering studies of binary mixtures in silica gels. Phys Rev E 51:5866-5879

Fu H, Trouw F, Sokol PE (1999) A quasi-elastic and inelastic neutron scattering study of H_2 in zeolite. J Low Temp Phys 116:149-165

Gaballa GA, Neilson GW (1983) The effect of pressure on the structure of light and heavy water. Molec Phys 50:97-111

Gallo P, Rovere M (2003) Anomalous dynamics of confined water at low hydration. J Phys Condens Matt 15: 7625-7633

Gay-Duchosal M, Powell DH, Lechner RE, Rufflé B (2000) QINS studies of water diffusion in Na-montmorillonite. Physica B 276-278:234-235
Geidel E, Lechert H, Döbler J, Jobic H, Calzaferri G, Bauer F (2003) Characterization of mesoporous materials by vibrational spectroscopic techniques. Micro Mesopor Mater 65:31-42
Glanville YJ, Pearce JV, Sokol PE, Newalker B, Komarneni S (2003) Study of H_2 confined in the highly ordered pores of MCM-48. Chem Phys 292:289-293
Gorbaty YE, Demianets YN (1983) The pair correlation functions of water at a pressure of 1000 bar in the temperature range 25-500 °C. Chem Phys Lett 100:450-454
Gorbaty YE, Kalinichev AG (1995) Hydrogen bonding in supercritical water. I. Experimental results. J Phys Chem 99:5336-5340
Gorbaty YE, Okhulkov AV (1994) High-pressure X-ray cell for studying the structure of fluids with the energy-dispersive technique. Rev Sci Inst 65:2195-2198
Goyal R, Fitch AN, Jobic H (2000) Powder neutron and X-ray diffraction studies of benzene adsorbed in zeolite ZSM-5. J Phys Chem B 104:2878-2884
Hahn RL, Narten AH, Annis BK (1986) Neutron scattering from solutions: The hydration of lanthanide and actinide ions. J Less-Common Metals 122:233-240
Hall PL, Ross DK (1981) Incoherent neutron-scattering functions for random jump diffusion in bounded and infinite media. Mol Phys 42:673-682
Halperin BI, Nelson DR (1978) Theory of two-dimensional melting. Phys Rev Lett 41:121-124
Hansen FY, Taub H (1999) The mechanism of melting in monolayer films of short and intermediate-length n-alkanes adsorbed on graphite. Inorg Mater 35:586-593
Hart RT, Benmore CJ, Neuefeind J, Kohara S, Tomberli B, Egelstaff PA (2005) Temperature dependence of isotopic quantum effects in water. Phys Rev Lett 94:047801-1 – 047801-4
Head-Gordon T, Hura G (2002) Water structure from scattering experiments and simulation. Chem Rev 102: 2651-2670
Helm L, Foglia F, Kowall T, Merbach AE (1994) Structure and dynamics of lanthanide ions and lanthanide complexes in solution. J Phys Condens Matter 6:A137-A140
Hempelmann R (2000) Quasielastic Neutron Scattering and Solid State Diffusion (Oxford Series on Neutron Scattering in Condensed Matter). Oxford University Press
Henson NJ, Eckert J, Hay PJ, Redondo A (2000) Adsorption of ethane and ethene in Na-Y studied by inelastic neutron scattering and computation. Chem Phys 261:111-124
Herdman GJ, Neilson GW (1990) Neutron scattering studies of aqua-ions. J Molec Liq 46:165-179
Herwig KW, Fuhrmann D, Criswell L, Taub H, Hansen FY, Dimeo R, Neumann DA (2000) Dynamics of intermediate-length alkane films adsorbed on graphite. J Phys IV 10:157-160
Hewish NA, Neilson GW, Enderby JE (1982) Environment of Ca^{2+} ions in aqueous solvent. Nature 297:138-139
Horita H, Cole DR (2004) Chapter 9. Stable isotope partitioning in aqueous and hydrothermal systems at elevated temperatures. *In*: Aqueous Systems at Elevated Temperatures and Pressures: Physical Chemistry in Water, Steam and Hydrothermal Solutions. Palmer DA, Fernández-Prini R, Harvey AH (eds) Elsevier, p 277-319
Howell I, Neilson GW (1997) Ni^{2+} coordination in concentrated aqueous solutions. J Molec Liq 73,74:337-348
Howell I, Neilson GW, Chieux P (1991) Neutron diffraction studies of ions in aqueous solution. J Molec Struct 250:281-289
Hura G, Sorensen JM, Head-Gordon T (2000) A high-quality X-ray scattering experiment in liquid water at ambient conditions. J Chem Phys 113:9140-9148
Ichikawa K, Kameda Y, Yamaguchi T, Wakita H, Misawa M (1991) Neutron-diffraction investigation of the intramolecular structure of a water molecule in the liquid phase at high temperatures. Molec Phys 73: 79-86
Idziak SHJ, Li Y (1998) Scattering studies of complex fluids in confinement. Curr Opin Colloid Interface Sci 3:293-298
Indris S, Heitjans P, Behrens H, Zorn R, Frick B (2005) Fast dynamics of H_2O in hydrous aluminosilicate glasses studied with neutron quasielastic scattering. Phys Rev B 71:064205-1-064205-9
Jobic H (1992) Molecular motions in zeolites. Spectrochem Acta A 48:293-312
Jobic H (2000a) Diffusion of linear and branched alkanes in ZSM-5. A quasi-elastic neutron scattering study. J Mol Calal A 158:135-142
Jobic H (2000b) Inelastic scattering of organic molecules in zeolites. Physica B 276:222-225
Jobic H, Bée M, Kärger J, Vartapetian RS, Balzer C, Julbe A (1995) Mobility of cyclohexane in a microporous silica sample: a quasi-elastic neutron scattering and NMR pulsed-field gradient technique study. J Membr Sci 108:71-78
Jobic H, Bée M, Pouget S (2000a) Diffusion of benzene in ZSM-5 measured by neutron spin-echo technique. J Phys Chem B 104:7130-7133

Jobic H, Czjzek M, van Santen RA (1992) Interaction of water with hydroxyl groups in H-mordenite: a neutron inelastic scattering study. J Phys Chem 96:1540-1542
Jobic H, Fitch AN, Combet J (2000b) Diffusion of benzene in NaX and NaY zeolites studied by quasi-elastic neutron scattering. J Phys Chem B 104:8491-8497
Jobic H, Kärger J, Bée M (1999) Simultaneous measurement of self- and transport diffusivities in zeolites. Phys Rev Lett 82:4260-4263
Jobic H, Paoli H, Méthivier A, Ehlers G, Kärger J, Krause C (2003) Diffusion of *n*-hexane in 5A zeolite studied by the neutron spin-echo and pulsed-field gradient NMR techniques. Micro Mesopor Mater 59:113-121
Jobic H, Tuel A, Krossner M, Sauer J (1996) Water interaction with acid sites in H-ZSM-5 zeolite does not form hydroxonium ions. A comparison between neutron scattering results and ab initio calculations. J Phys Chem 100:19545-19550
Johnson MR, Kearley GI (2000) Quantitative atom-atom potentials from rotational tunneling: their extraction and their use. Ann Rev Phys Chem 51:297-321
Kalinichev A (2001) Molecular simulations of liquid and supercritical water: Thermodynamics, Structure and hydrogen bonding. Rev Mineral Geochem 42:83-129
Kemner E, Overweg AR, Jayasooriya UA, Parker SF, de Schepper IM, Kearley GJ (2002) Ferrocene-zeolite interactions measured by inelastic neutron scattering. Appl Phys A 74:S1368-S1370
Kennedy D, Norman C (2005) What don't we know? Science 309:75-102
Kim HK, Zhang QM, Chan MH (1986) Experimental evidence of continuous melting of ethylene on graphite. Phys Rev Lett 56:1579-1582
Kittaka S, Takahara S, Yamaguchi T, Bellissent-Funel MC (2005) Interlayer water molecules in vanadium pentoxide hydrate. 8. Dynamic properties by quasi-elastic neutron scattering. Langmuir 21:1389-1397
Kjems J, Passell L, Taub H, Dash JG, Novaco AD (1976) Neutron scattering study of nitrogen adsorbed on basal plane oriented graphite. Phys Rev B 13:1446-1462
Knudsen KD, Fossum JO, Helgesen G, Bergaplass V (2003) Pore characteristics and water absorption in a synthetic smectite clay. J Appl Cryst 36:587-591
Kosterlitz JM, Thouless DJ (1973) Long range order and metastability in two dimensional solids and superfluids. J Phys C 6:1181
Larese JZ (1993) Multilayer argon films on graphite: structural and melting properties. Accounts Chem Res 26:353-360
Larese JZ (1997) Structure and dynamics of physisorbed phases. Solid State & Mat Sci 2:539-545
Larese JZ (1999) Neutron scattering investigations of the dynamics of thin films adsorbed on solid surfaces. Neutrons 57-68
Larese JZ, Frazier L, Arnold T, Hinde RJ, Ramirez-Cuesta AJ (2006) Direct observation of molecular hydrogen binding to magnesium oxide surfaces. Physica B (in press) doi: 10.1016/j.physb.2006.05.344
Larese JZ, Harada M, Passell L, Krim J, Satija S (1988a) Neutron scattering study of methane bilayer and trilayer films on graphite. Phys Rev B 37:4735-4742
Larese JZ, Passell L, Heidemann A, Richter D, Wicksted JP (1988b) Melting in two dimensions: The ethylene-on-graphite system. Phys Rev Lett 61:432-435
Larese JZ, y Marei DM, Sivia DS, Carlile CJ (2001) Tracking the evolution of interatomic potentials with high resolution inelastic neutron scattering. Phys Rev Lett 87:206102-1–206102-4
Leberman R, Soper AK (1995) Effect of high salt concentrations on water structure. Nature 378:364-366
Li JC, Ross DK, Howe LD, Stefanopoulos KL, Fairclough JPA, Heenan R, Ibel K (1994) Small-angle neutron scattering studies of the fractal-like network formed during desorption and adsorption of water in porous materials. Phys Rev B 49:5911-5917
Lin MY, Sinha SK, Drake JM, Wu X-I, Thiyagarajan P, Stanley HB (1994) Study of phase separation of binary fluid mixture in confined geometry. Phys Rev Lett 72:2207-2210
Line CMB, Winkler B, Dove MT (1994) Quasielastic incoherent neutron scattering study of the rotational dynamics of water molecules in analcime. Phys Chem Min 21:451-459
Liu L, Faraone A, Mou C-Y, Shih P-C, Chen SH (2004) Slow dynamics of supercooled water confined in nanoporous silica materials. J Phys Condens Matter 16:S5403-S5436
Loong C-K (2006) Inelastic scattering and applications. Rev Mineral Geochem 63:233-254
Loong CK, Price DL (1984) Hydrogen-bond spectroscopy of water by neutron scattering. Phys Rev Lett 53: 1360-1363
Maddox SA, Gomez P, McCall KR, Eckert J (2002) Water mobility in Calico Hills tuff measured by quasielastic neutron scattering. Geophys Res Lett 29:Art. No. 1259, doi: 10.1029/2001Glv14167
Malikova N, Gadéne A, Marry V, Dubois E, Turq P (2006) Diffusion of water in clays on the microscopic scale: Modeling and experiment. J Phys Chem B 110:3206-3214
Malikova N, Gadéne A, Marry V, Dubois E, Turq P, Zanotti J-M, Longeville S (2005) Diffusion of water in clays – microscopic simulation and neutron scattering. Chem Phys 317:226-235
Mamontov E (2004) Dynamics of surface water in ZrO_2 studied by quasielastic neutron scattering. J Chem Phys 121:9087-9097

Mamontov E (2005) High-resolution neutron scattering study of slow dynamics of surface water molecules in zirconium oxide. J Chem Phys 123:024706-1 – 024706-9
Mamontov E, Kumzerov YA, Vakhrushev SB (2005a) Diffusion of benzene confined in the oriented nanochannels of chrysotile asbestos fibers. Phys Rev E 72:051502-1-051502-7
Mamontov E, Kumzerov YA, Vakhrushev SB (2005b) Translational dynamics of water in the nanochannels of oriented chrysotile asbestos fibers. Phys Rev E 71:061502-1 – 061502-5
Mansour F, Dimeo RM, and Peemoeller H (2002) High resolution inelastic neutron scattering from water in mesoporous silica. Phys Rev E 66:041307-1 – 041307-7
Mellot CF, Davidson AM, Eckert J, Cheetham AK (1998) Adsorption of chloroform in NaY zeolite: A computational and vibrational spectroscopy study. J Phys Chem B 102:2530-2535
Melnichenko YB, Schüller J, Richter R, Ewen B, Loong C-K (1995) Dynamics of hydrogen-bonded liquids confined to mesopores: a dielectric and neutron spectroscopy study. J Chem Phys 103:2016-2024
Melnichenko YB, Wignall GD, Cole DR, Frielinghaus H (2004) Density fluctuations near the liquid-gas critical point of a confined fluid. Phys Rev E 69:057102-1-057102-4
Melnichenko YB, Wignall GD, Cole DR, Frielinghaus H (2006) Adsorption of supercritical CO_2 in aerogels as studied by small-angle neutron scattering and neutron transmission techniques. J Chem Phys 124: 204711-1 – 204711-11
Melnichenko YB, Wignall GD, Cole DR, Frielinghaus H, Bulavin LA (2005) Liquid-gas critical phenomena under confinement: small-angle neutron scattering studies of CO_2 in aerogel. J Molec Liq 120:7-9
Messe L, Perdigon A, Clarke SM, Inaba A, Arnold T (2005) Alkane-alcohol mixed monlayers at the solid/ liquid interface. Langmuir 21:5085-5093
Michielsen JCF, Bot A, van der Elsken J (1988) Small-angle X-ray scattering from supercooled water. Phys Rev A 38:6439-6441
Mitchell PCH, Parker SF, Ramirez-Cuesta AJ, Tomkinson J (2005) Vibrational Spectroscopy with Neutrons. World Scientific
Mitchell PCH, Tomkinson J, Grimblot JG, Payen E (1993) Bound water in aged molybdate alumina hydrodesulfurization catalysts – an inelastic neutron scattering study. Faraday Trans 89:1805-1807
Mitra S, Mukhopadhyay R (2003) Molecular dynamics using quasielastic neutron scattering technique. Curr Sci 84:653-662
Mitra S, Mukhopadhyay R, Pillai KT, Vaidya VN (1998) Diffusion of water in porous alumina: neutron scattering study. Solid State Commun 105:719-723
Mitra S, Mukhopadhyay R, Tsukushi I, Ikeda S (2001) Dynamics of water in confined space (porous alumina): QENS study. J Phys Condens Matter 13:8455-8465
Nair S, Chowdhuri Z, Peral I, Neumann DA, Dickinson LC, Tompsett G, Jeong H-K, Tsapatsis M (2005) Translational dynamics of water in a nanoporous layered silicate. Phys Rev B 71:104301-1-104301-8
Neilson GW, Adya AK (1997) Neutron diffraction studies on liquids. Ann Rep Prog Chem- Phys Chem, Sect C 93:101-145
Neilson GW, Adya AK, Ansell S (2002) Neutron and X-ray diffraction studies on complex liquids. Annu Rep Prog Chem- Phys Chem Sect C 98:273-322
Neilson GW, Broadbent RD (1990) The structure of Sr^{2+} in aqueous solution. Chem Phys Lett 167:429-431
Neilson GW, Broadbent RD, Howell I, and Tromp RH (1993) Structural and dynamical aspects of aqueous ionic solutions. J Chem Soc Faraday Trans 89:2927-2936
Neilson GW, Enderby JE (1989) The coordination of metal aquaions. Adv Inorg Chem 34:195-218
Neilson GW, Enderby JE (1996) Aqueous solutions and neutron scattering. J Phys Chem 100:1317-1322
Neilson GW, Mason PE, Ramos S, Sullivan D (2001) Neutron and X-ray scattering studies of hydration in aqueous solutions. Phil Trans R Soc London A 359:1575-1591
Neilson GW, Page DI, Howell WS (1979) A neutron diffraction study of the structure of heavy water at pressure using a new high-pressure cell. J Phys D: Appl Phys 12:901-907
Neilson GW, Skipper NT (1985) Potassium (1+) ion coordination in aqueous solution. Chem Phys Lett 114: 35-38
Neumann DA (2006) Neutron scattering and hydrogenous materials. Mater Today 9:34-41
Newsome JR, Neilson GW, Enderby JE (1980) Lithium ions in aqueous solution. J. Phys C-Solid State Phys 13:L923-L926
Ohtaki H, Radnai T (1993) Structure and dynamics of hydrated ions. Chem Rev 93:1157-1204
Paoli H, Méthivier A, Jobic H, Krause C, Pfeifer H, Stallmach F, Kärger J (2002) Comparative QENS and PFG NMR diffusion studied of water in zeolite NaCaA. Micro Mesopor Mater 55:147-158
Papadopoulos GK, Jobic H, Theodorou DN (2004) Transport diffusivity of N_2 and CO_2 in silicalite: coherent quasielastic neutron scattering measurements and molecular dynamics simulations. J Phys Chem B 108: 12748-12756
Petrillo C, Sacchetti F, Dorner B, Suck JB (2000) High-resolution neutron scattering measurement of the dynamic structure factor of heavy water. Phys Rev E 62:3611-3618

Phillips JM, Zhang QM, Larese JZ (1993) Why do vertical steps reappear in adsorption isotherms? Phys Rev Lett 71:2971-2974

Pitteloud C, Powell DH, Fischer HE (2001) The hydration structure of the Ni^{2+} ion intercalated in montmorillonite clay: a neutron diffraction with isotopic substitution study. Phys Chem Chem Phys 3: 5567-5574

Pitteloud C, Powell DH, Gonzalez MA, Cuello GJ (2003) Neutron diffraction studies of ion coordination and interlayer water structure in smectite clays: lanthanide(III)-exchanged Wyoming montmorillonite. Colloids Surf A 217:129-136

Pitteloud C, Powell DH, Soper AK, Benmore CJ (2000) The structure of interlayer water in Wyoming montmorillonite studied by neutron diffraction with isotropic substitution. Physica B 276-278:236-237

Postorino P, Tromp RH, Ricci MA, Soper AK, Neilson GW (1993) The interatomic structure of water at supercritical temperatures. Nature 366:668-670

Powell DH, Fischer HE, Skipper NT (1998) The structure of interlayer water in Li-montmorillonite studied by neutron diffraction with isotopic substitution. J Phys Chem B 102:10899-10905

Powell DH, Neilson GW, Enderby JE (1989) A neutron diffraction study of $NiCl_2$ in D_2O and H_2O. A direct determination of $g_{NiH}(r)$. J Phys-Condens Matt 1:8721-8733

Powell DH, Neilson GW, Enderby JE (1993) The structure of Cl^- in aqueous solutions: an experimental determination of $g_{ClH}(r)$ and $g_{ClO}(r)$. J Phys Condens Matter 5:5723-5730

Press W (1981) Single-Particle Rotations in Molecular Crystals. Springer Tracts in Modern Physics, Vol 92. Springer

Proffen T (2006) Analysis of disordered materials using total scattering and the atomic pair distribution function. Rev Mineral Geochem 63:255-274

Radlinski AP (2006) Small-angle neutron scattering and the microstructure of rocks. Rev Mineral Geochem 63:363-397

Ramsay JDF (1998) Surface and pore structure characterization by neutron scattering techniques. Adv Colloid Interf Sci 76-77:13-37

Ricci MA, Bruni F, Gallo P, Rovere M, Soper AK (2000) Water in confined geometries: experiments and simulations. J Phys Condens Matt 12:A345-A350

Ricci MA, Soper AK (2002) Jumping between water polymorphs. Phys A 304:43-52

Rosi NL, Eckert J, Eddaoudi M, Vodak DT, Kim J, O'Keeffe M, Yaghi OM (2003) Hydrogen storage in microporous metal-organic frameworks. Science 300:1127-1129

Schenkel R, Jentys A, Parker SF, Lercher JA (2004a) INS and IR and NMR spectroscopic study of C-1-C-4 alcohols adsorbed on alkali metal-exchanged zeolite X. J Phys Chem B 108:15013-15026

Schenkel R, Jentys A, Parker SF, Lercher JA (2004b) Investigation of the adsorption of methanol on alkali metal cation exchanged zeolite X by inelastic neutron scattering. J Phys Chem B 108:7902-7910

Simon Ch, Rosenman I, Batallan F, Rogerie J, Legrand JF, Magerl A, Lartigue C, Fuzellier H (1990) Measurement of defect mobility in a defect-mediated melting. Phys Rev B 41:2390-2397

Singwi KS, Sjölander A (1960) Diffusive motions in water and cold neutron scattering. Phys Rev 119:863-871

Skipper NT, Lock PA, Titiloye JO, Swenson J, Zakaria AM, Spencer Howells W, Fernadez-Alonso F (2006) The structure and dynamics of 2-dimensional fluids in swelling clays. Chem Geol 230:182-196

Skipper NT, Neilson GW, Cummings SC (1989) An X-ray diffraction study of aquated nickel (2+) and magnesium (2+) by difference methods. J Phys-Condens Matt 1:3489-3506.

Skipper NT, Smalley MV, Williams GD, Soper AK, Thompson CH (1995) Direct measurement of the electric double-layer structure in hydrated lithium vermiculite clays by neutron diffraction. J Phys Chem 99: 14201-14204

Skipper NT, Soper AK, McConnell JDC (1990) The structure of interlayer water in vermiculite. J Chem Phys 94:5751-5760

Skipper NT, Soper AK, Smalley MV (1994) Neutron diffraction study of calcium vermiculite: hydration of calcium ions in a confined environment. J Phys Chem 98:942-945

Soper AK (1996) Bridge over troubled water: the apparent discrepancy between simulated and experimental non-ambient water structure. J Phys Condens Matter 8:9263-9267

Soper AK (2000) The radial distribution functions of water and ice from 220 to 673 K and at pressures up to 400 MPa. Chem Phys 258:121-137

Soper AK (2005) Partial structure factors from disordered materials diffraction data: An approach using empirical potential structure refinement. Phys Rev B 72:104204(1)-104204(12)

Soper AK, Bruni F, Ricci MA (1997) Site-site pair potential functions of water from 25 to 400°C: Revised analysis of old and new diffraction data. J Chem Phys 106:247-254

Soper AK, Egelstaff PA (1981) The structure of liquid hydrogen chloride. Molec Phys 42:399-410

Soper AK, Phillips MG (1986) A new determination of the structure of water at 25°C. Chem Phys 107:47-60

Soper AK, Silver RN (1982) Hydrogen-hydrogen pair correlation function in liquid water. Phys Rev Lett 49: 471-474

Soper AK, Turner J (1993) Impact of neutron scattering on the study of water and aqueous solutions. Int J Modern Phys B 7:3049-3076

Sorensen JM, Hura G, Glaeser RM, Head-Gordon T (2000) What can X-ray scattering tell us about the radial distribution functions of water. J Chem Phys 113:9149-9161

Stanley HE, Teixeira J (1980) Interpretation of the unusual behavior of H_2O and D_2O at low temperatures: tests of a percolation theory. J Chem Phys 73:3404-3422

Stepanov AG, Shegai TO, Luzgin MV, Jobic H (2003) Comparison of the dynamics of *n*-hexane in ZSM-5 and 5A zeolite structures. Eur Phys J E 12:57-61

Stephens PW, Heiney PA, Birgeneau RJ, Horn PM, Moncton DE, Brown GE (1984) High resolution X-ray scattering study of the commensurate-incommensurate transition of monolayer Kr on graphite. Phys Rev B 29:3512-3532

Steytler DC, Dore JC, Wright CJ (1983) Neutron diffraction study of cubic ice nucleation in a porous silica network. J Phys Chem 87:2458-2459

Strandberg KJ (1988) Two dimensional melting. Rev Mod Phys 60:161-207

Swenson J, Bergman R, and Howells WS (2000) Quasielastic neutron scattering of two-dimensional water in a vermiculite clay. J Chem Phys 113:2873-2879

Swenson J, Bergman R, Longeville S (2001a) A neutron spin-echo study of confined water. J Chem Phys 115: 11299-11305

Swenson J, Bergman R, Longeville S, Howells WS (2001b) Dynamics of 2D-water as studied by quasi-elastic neutron scattering and neutron resonance spin-echo. Physica B 301:28-34

Swenson J, Jansson H, Howells WS, Longeville S (2005) Dynamics of water in a molecular sieve by quasielastic neutron scattering. J Chem Phys 122:084505-1-084505-7

Takahara S, Kittaka S, Kuroda Y, Yamaguchi T, Fujii H, Bellissent-Funel MC (2000) Interlayer water molecules in vanadium pentoxide hydrate, $V_2O_5{\cdot}nH_2O$. Part 7. Quasi-elastic neutron scattering study. Langmuir 16:10559-10563

Takahara S, Nakano M, Kittaka S, Kuroda Y, Mori T, Hamano H, Yamaguchi T (1999) Neutron scattering study on dynamics of water molecules in MCM-41. J Phys Chem B 103:5814-5819

Takahara S, Sumiyama N, Kittaka S, Yamaguchi T, Bellissent-Funel MC (2005) Neutron scattering study on dynamics of water molecules in MCM-41. 2. Determination of translational diffusion coefficient. J Phys Chem B 109:11231-11239

Takamuku T, Yamagami M, Wakita H, Masuda Y, Yamaguchi T (1997) Thermal property, structure, and dynamics of supercooled water in porous silica by calorimetry, neutron scattering, and NMR relaxation. J Phys Chem B 101:5730-5739

Tassaing T, Bellissent-Funel MC (2000) The dynamics of supercritical water: A quasielastic incoherent neutron scattering study. J Chem Phys 113:3332-3337

Tassaing T, Bellissent-Funel MC, Guillot B, Guissani Y (1998) The partial pair correlation functions of dense supercritical water. Europhys Lett 42:265-270

Taub H, Torzo G, Lauter HJ, Fain SF (eds) (1991) Phase Transitions in Surface Films 2, Vol 267. NATO Adv Study Inst Series B: Physics. Plenum

Teixeira J, Bellissent-Funel MC, Chen SH, Dianoux AJ (1985) Experimental determination of the nature of diffusive motions of water molecules at low temperature. Phys Rev A 31:1913-1917

Thiessen WE, Narten AH (1982) Neutron diffraction study of light and heavy water mixtures at 25°C. J Chem Phys 77:2656-2662

Tromp RH, Neilson GW (1996) Neutron diffraction study of the hydration of ions in aqueous ion exchange resins. J Phys Chem 100:7380-7383

Tromp RH, Neilson GW, Soper AK (1992) Water-structure in concentrated lithium chloride solutions. J Chem Phys 96:8460-8469

Tromp RH, Postorino P, Neilson GW, Ricci MA, Soper AK (1994) Neutron diffraction studies of H_2O/D_2O at supercritical temperatures. A direct determination of $g_{HH}(r)$, $g_{OH}(r)$, and $g_{OO}(r)$. J Chem Phys 101: 6210-6215

Uffindell CH, Kolesnikov AI, Li JC, Mayers J (2000) Inelastic neutron scattering study of water in the subcritical and supercritical region. Phys Rev B 62:5492-5495

Venturini F, Gallo P, Ricci MA, Bizzarri AR, Cannistraro S (2001) Low frequency scattering excess in supercooled confined water. J Chem Phys 114:10010-10014

Venuti V, Crupi V, Majolino D, Migliardo P, Bellissent-Funel MC (2004) Neutron diffraction study of structure of water confined in a sol-gel silica glass. Physica B 350:E599-E601

Walrafen GE, Wang WH, Chu YC (1999) Raman spectra from saturated water vapor to the supercritical fluid. J Phys Chem B 103:1332-1338

Walton RI, Francis RJ, Halasyamani PS, O'Hare D, Smith RI, Done R, Humphreys RJ (1999) Novel apparatus for the *in situ* study of hydrothermal crystallizations using time-resolved neutron diffraction. Rev Sci Instr 70:3391-3396

Walton RI, Norquist A, Smith RI, O'Hare D (2002) Recent results from the *in situ* study of hydrothermal crystallizations using time-resolved X-ray and neutron diffraction methods. Faraday Disc 122:331-341

Wang J, Kalinichev AG, Kirkpatrick RJ (2006) Effects of substrate structure and composition on the structure, dynamics, and energetic of water at mineral-surfaces: A molecular dynamics modeling study. Geochim Cosmochim Acta 70:562-582

Warren BE (1941) X-ray diffraction in random layer lattices. Phys Rev 59:693-698

Webber JBW, Dore JC, Fischer H, Vuillard L (1996) Critical scattering by fluid cyclohexane in porous silica. Chem Phys Lett 253:367-371

Wernet Ph, Nordlund D, Bergmann U, Cavalleri M, Odelius M, Ogasawara H, Naslund LA, Hirsch TK, Ojamac L, Glatzel P, Petersson LGM, Nilsson A (2004) The structure of the first coordination shell in liquid water. Science 304:995-999

Wesolowski DJ, Ziemniak SE, Anovitz LM, Machesky ML, Bénézeth P, Palmer D.A. (2004) Solubility and surface adsorption characteristics of metal oxides. *In*: Aqueous Systems at Elevated Temperatures and Pressures: Physical Chemistry in Water, Steam and Hydrothermal Solutions. Palmer DA, Fernández-Prini, Harvey AH (eds) Elsevier, p 493-595

Wilding MC, Benmore CJ (2006) Structure of glasses and melts. Rev Mineral Geochem 63:275-311

Williams GD, Skipper NT, Smalley MV (1997) Isotope substitution of interfacial fluids in vermiculite clays. Physica B 234-236:375-376

Williams GD, Soper AK, Skipper NT, Smalley MV (1998) High-resolution structural study of an electrical double layer by neutron diffraction. J Phys Chem B 102:8945-8949

Williams Q, Hemley RJ (2001) Hydrogen in the deep Earth. Annual Rev Earth Planet Sci 29:365-418

Wilson JE, Ansell S, Enderby JE, Neilson GW (1997) Water structure around chloride ions in the presence of biologic macromolecule. Chem Phys Lett 278:21-25

Winter R (1993) Neutron and X-ray scattering of fluids at high pressure and high temperature. *In:* High Pressure Chemistry, Biochemistry and Materials Science. Winter R, Jonas J (eds) Springer, p 167-199

Yamaguchi T (1998) Structure of subcritical and supercritical hydrogen-bonded liquids and solutions. J Molec Liq 78:43-50

Yamanaka K, Yamaguchi T, Wakita H (1994) Structure of water in the liquid and supercritical states by rapid x-ray diffractometry using an imaging plate detector. J Chem Phys 101:9830-9836

Young AP (1979) Melting and the vector Coulomb gas in two dimensions. Phys Rev B 19:1855-1866

Zangi R (2004) Water confined to a slab geometry: a review of recent computer simulation studies. J Phys Condens Matt 16:S5371-S5388

Zanotti J-M, Bellissent-Funel MC, Chen SH (1999) Relaxational dynamics of supercooled water in porous glass. Phys Rev E 59:3084-3093